7

Ultrasonic Imaging in Liver Disease: From Bench to Bedside

Celia Resende, Andréia Lessa and Regina C. S. Goldenberg
Universidade Federal do Rio de Janeiro
Brazil

1. Introduction

Hepatology is an excellent example of how results deriving from basic science influence our everyday clinical practice. This involves diagnostic procedures as well as therapeutic developments. The role of diagnostic imaging in the assessment of liver disease continues to gain in importance. Imaging of the liver has progressed rapidly during the past decade with continued advancement of current ultrasound, computed tomography, and magnetic resonance imaging. Refinement enabling better anatomic characterization of disease and significant strength from the addition of new techniques and high resolution images were seen. Improvements in ultrasound (US) scanners over the past few decades have been remarkable: advances such as color Doppler and harmonic imaging have increased image quality and accuracy. Ultrasound is usually the first imaging modality in the evaluation of liver disease because it is easy to perform, widely available, relatively inexpensive and is cost effective. US can detect morphological changes in the liver and characterize focal lesions (cystic or solid) with high accuracy. Color Doppler sonography is a well established method for assessment of the hepatic vasculature, offering hemodynamic and anatomical information.

2. Hepatic ultrasound in rodents

An important challenge in pre-clinical *in vivo* studies is to follow up the evolution of the disease induced in animal models without sacrifice them. In this context, noninvasive methods available for the diagnosis and prognosis of liver diseases bring a significant contribution for the progress of this field of study. Prior animal research may support the step forward to human clinical trials.

Rodents represent an important animal group used in experimental model of liver diseases. Steatosis, cirrhosis and some hepatic focal lesions can be induced in mice and rats by administration of toxins, among which carbon tetrachloride (CCL4), ally alcohol, retrorsine and 2-acetylaminofluorene (2-AAF), by surgical insult such as bile duct ligation or hepatic resection, and virus infection. The induced hepatopathies may present change in liver size, shape, position, or opacity and these parameters can be evaluated by ultrasound imaging.

US imaging is an ideal complementary diagnostic tool to evaluate the liver. Hepatic ultrasound can noninvasively examine the internal architecture of the liver parenchyma, biliary system, portal and hepatic vascular supply. Also, ultrasonography allows assessment

of changes in liver echogenicity, which correlates with disease (Lessa et al., 2010); identifies focal verses diffuse disease processes (Lima et al., 2008); detects vascular and biliary abnormalities (Partington & Biller, 1995). Additionally, besides being a noninvasive method, US is innocuous, reliable, rapid, reproducible and inexpensive, with high accuracy in evaluating liver disease.

2.1 Scanning techniques for hepatic ultrasound in rodents

Tranquilization is always required. In our experience, animals are successfully anesthetized using Ketamine (0.5mL/kg) and Xilazin (1mL/kg) intraperitoneally or by inhalation of Isoflurane, USP. If possible, the rodent should be fasting for 12 hours. This preparation may prevent vomiting and aspiration during anesthesia and helps reducing the sonographic barriers of excessive gas in the stomach and intestine.

The ventral abdomen must be shaved or have the hair removed with a commercially available hair remover creme to reduce imaging artifacts in the ultrasonographic examination. A sound-conducting gel is applied and the US examination can be performed in rats using a multifrequencial linear transducer (7.5 to 12MHz) attached to a conventional ultrasound machine or can be performed in mice and in rats using mechanical sector high resolution transducers (30 MHz and 40 MHz) in a dedicated ultrasound equipment for small animals (Vevo 770 - Visualsonics – Canada).

The animals are positioned in dorsal recumbence on a rectangular table for liver, hepatic artery and portal vein scanning. The liver is assessed by placing the transducer just distal to the last right costal cartilages and angling its beam cranially, obtaining multiple transversal and longitudinal scans (Fig. 1A-D). The hepatic artery and portal vein are scanned in the longitudinal views.

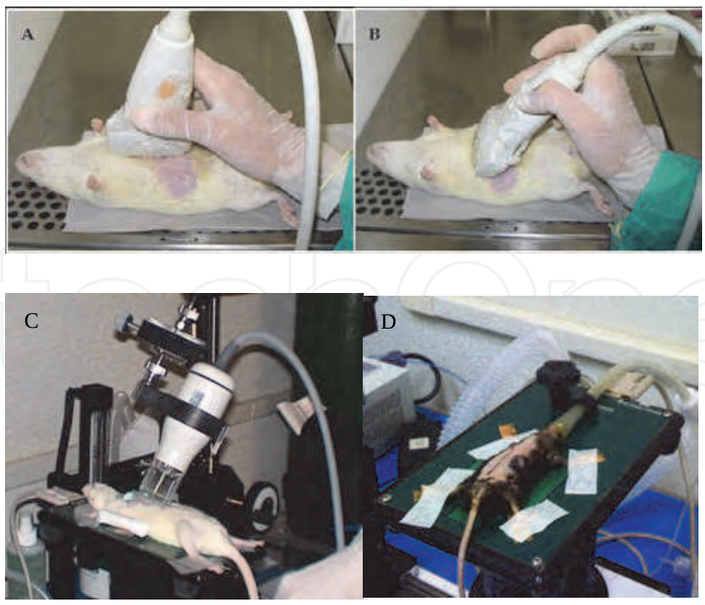

Fig. 1. Liver scanning: [1.A] Longitudinal scans are made by angling the transducer beam from right to left; [1.B] Transversal scans are made by angling the transducer beam from cranial to caudal; [1.C] High resolution mechanical sector transducer; [1.D] Dedicated ultrasound table with inhalatory anesthesia system.

2.2 The normal hepatic ultrasound

In order to standardize normal US parameters, our research group has examined 276 healthy Wistar rats. Such as described in small animals, the liver is bounded cranially by the concave highly echogenic curvilinear structure of the diaphragm-lung interface. It is bordered caudally by the fluid and gas reverberations in the fundus and body of the stomach to the left, and the pylorus and right kidney to the right. The anatomy divides the rat liver in four lobes: the right lateral lobe, middle, left lateral and caudate lobes, which in turn have independent portal and arterial vascularization and a separate biliar drainage. The right lateral lobe is subdivided into two segments, anterior and posterior, the last one adjacent to the right kidney and placed behind the inferior vena cava. The left lateral lobe is located on the left, in front of the stomach. In the midline, the caudate lobe is located dorsally and the median lobe lies ventrally.

The liver has homogeneous parenchyma with medium level echogenicity and straight hepatic surface as normal characteristics (Fig. 2A) (Dias et al., 2008; Lessa et al., 2010; Manheimer et al., 2009). In the 276 rats we examined, the transverse diameter of the liver measures from 3.5 to 3.8 cm and the portal vein caliber between 1.5 mm and 1.6 mm. The hepatic parenchyma is less echogenic than the right renal cortex in the great majority of rodents. Similar echogenicity in both organ parenchymas is observed in less than 5% of them (Lessa et al., 2008). The ultrasonographer should attempt to obtain images of the liver adjacent to the right kidney (longitudinal scan) (Fig. 2B). These images have to be made with proper control settings to prevent an incorrect diagnosis of diffuse hepatic disease. The hepatic parenchyma contains variably sized circular and tubular anechoic structures that represent the hepatic and portal veins (Partington & Biller, 1995).

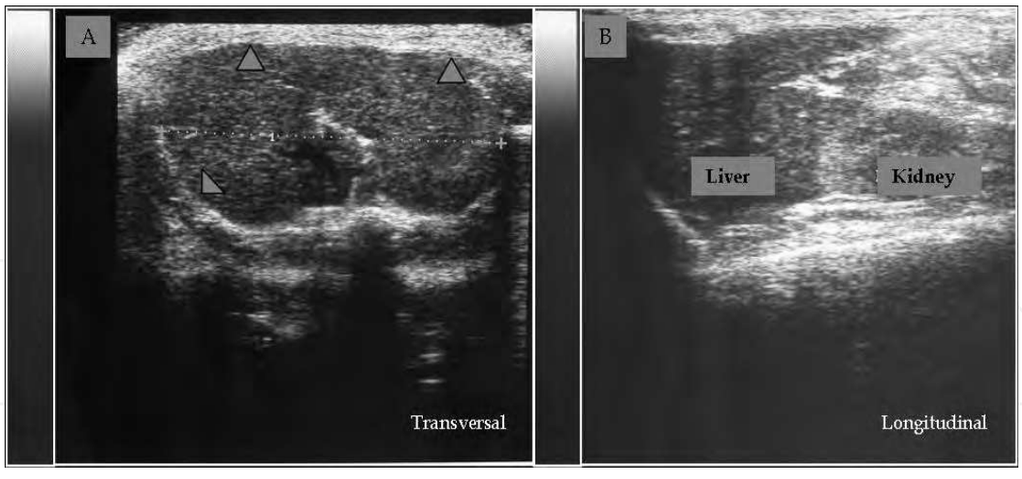

Fig. 2. Liver sonograms of a healthy rat: [2.A] Transversal sonogram shows homogeneous liver parenchyma, with medium level echogenicity and a regular hepatic surface (arrowheads); [2.B] Longitudinal sonogram presents right renal cortex more echogenic than liver parenchyma.

The caudal vena cava and the portal vein are parallel and run longitudinally. The portal vein caliber is measured in the mid-point of the main portal vein (Fig. 3A). Intrahepatic bile ducts are not identified routinely with ultrasound. Rats do not have gallbladder but mice do have it. The spleen has a homogeneous parenchyma (Fig.3B).

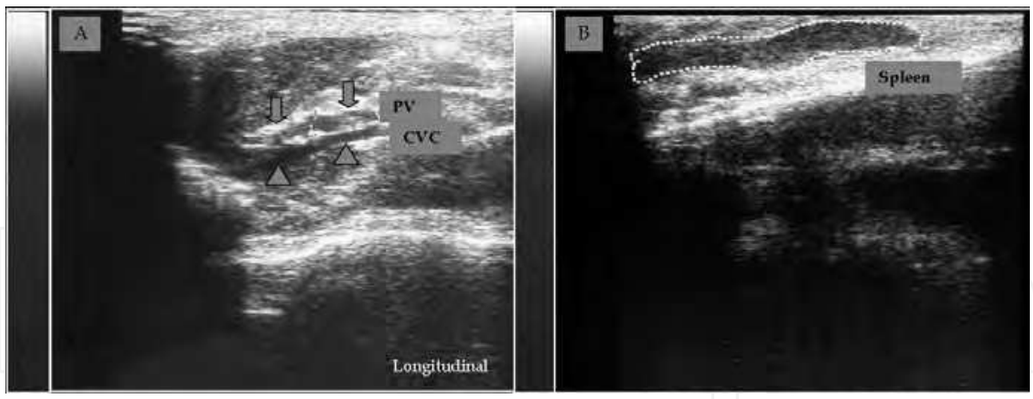

Fig. 3. [3.A] Longitudinal sonogram: portal vein (PV) (arrows) and the caudal vena cava (CVC) (arrowheads) in a healthy rat; [3B] Spleen sonogram: measurement of its area.

In high resolution ultrasound equipment specially designed to evaluate small animals the liver parenchyma and the relationship between liver/kidney echogenicity in rodents can be accurately examined. The portal vein caliber of the mice measures around 1.0 mm and the hepatic artery around 0.2 mm. This equipment allows to use the Doppler method to evaluate vascular resistance. The hepatic artery has a normal low resistance flow with the resistive index (RI) measuring around 0.50 (Fig. 4A-C). Resistive index (RI) is calculated using the peak systolic velocity (S) and end diastolic velocity (D) measurements as follows:

$$RI=\frac{S-D}{S}$$

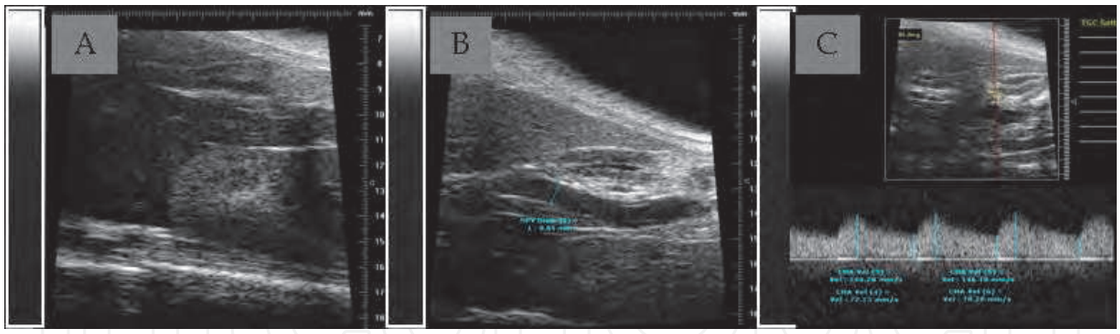

Fig. 4. [4.A] Longitudinal scan: normal liver parenchyma less echogenic than the renal cortex. [4B] Longitudinal scan: normal portal vein (PV) - caliber: 0.85 mm. [4C] Doppler spectrum: normal low resistance flow of the hepatic artery with high diastolic flow.

2.3 Difuse hepatic disease

Difuse hepatic disease may cause a change in the echogenicity of hepatic parenchyma (Dias et al., 2008; Lessa et al., 2010). Increased echogenicity is identified as hepatic echogenicity equal or greater than the renal cortex and similar to the spleen (Lessa et al., 2010; Lima et al., 2008; Partington & Biller, 1995). Diseases that may cause an increase in hepatic echogenicity include cirrhosis, hepatic steatosis, steroid hepatopathy, lymphosarcoma, and long-term cholangiohepatitis (Partington & Biller, 1995).

In 2005, Lee et al. demonstrated that B-mode mean grey level has a close correlation with fatty change and it is useful for the diagnosis of liver fibrosis (Lee et al., 2005). In 2008, it was described that US revealed steatosis based on liver echogenicity relative to the kidney and could detect focal lesions up to 0.5 mm in a rat model of NASH (non-alcoholic steatohepatitis) with cirrhosis (Lima et al., 2008).

In 2010, our group determined the reliability of US findings in the assessment of fatty liver disease and cirrhosis in rats in comparison to histological results by following up a rat model of hepatic disease induced by dual exposure to CCl_4 and ethanol (Lessa et al., 2010). In brief, ultrasound analysis was performed after 4, 8 and 15 weeks of liver injury induction, following the scanning techniques for hepatic ultrasound in rodents described above. Ultrasonographic findings were analyzed based on our previous observations and on criteria for US diagnosis in humans according to the following classification:

A. Liver echogenicity (Fig. 5) - four patterns: (0) homogeneous liver parenchyma with medium level echogenicity and a regular hepatic surface; (1) diffusely increased parenchymal echogenicity, reduced visualization of the diaphragm and small peripheral vessels with no change on liver surface; (2) discrete coarse and heterogeneous parenchymal echogenicity, dotted or slightly irregular liver surface; (3) extensive coarse and heterogeneous parenchymal echogenicity, irregular or nodular hepatic surface with underlying regenerative nodules;

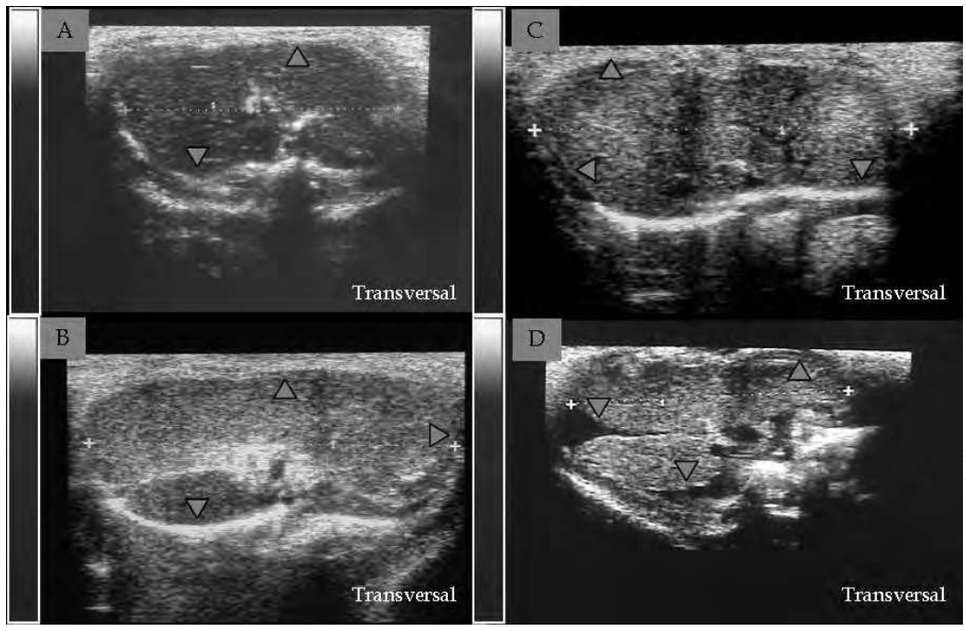

Fig. 5. Liver echogenicity patterns:
[5A] Pattern 0
[5B] Pattern 1
[5C] Pattern 2
[5D] Pattern 3

B. Inversion of the echographic relationship between the liver and the renal cortex (Fig. 6). This finding was considered to be positive if the echogenicity of the liver parenchyma was greater or equal to the right renal cortex, instead of lesser than it;

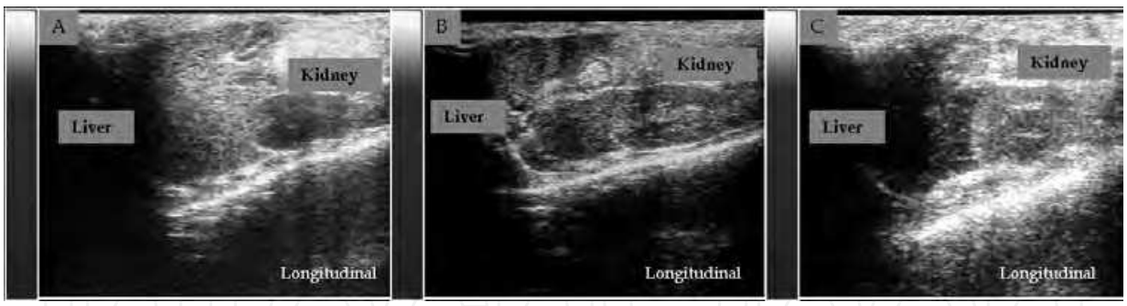

Fig. 6. Relationship between liver and right kidney echogenicities: Longitudinal scan [6A] Liver is less echogenic than right renal cortex; [6B] Hepatic echogenicity is equal to the right renal cortex in a cirrhotic liver; [6C] Hepatic parenchyma is more echogenic than right renal cortex in a steatotic liver.

C. Increased portal vein caliber (PVC). PVC was considered to be abnormal if equal or greater than 2.1 mm;
D. Presence of ascites;
E. Spleen area;
F. Doppler waveforms of the hepatic artery shows an increase in the resistive index due to the difficult inflow related to the presence of diffuse liver disease.

The liver parenchymal echogenicity changes correlates to the time of injury induction. The first pattern of liver echogenicity (pattern 0) is identified in normal rats. The pattern 1 correlates to fatty liver without/with minimal fibrosis. The pattern 2 corresponds to steatosis associated to different degrees of fibrosis and pattern 3 correlates to cirrhosis.

Cirrhosis may present nodules from macronodular regeneration (Lessa et al., 2010; Partington & Biller, 1995). As these nodules are most commonly isoechoic, their identification by ultrasound is difficult (Biller et al., 1992).

The hepatic echogenicity increases due to the presence of fatty infiltration and/or fibrosis, changing the relation between liver and right renal cortex (Biller et al., 1992). In our experience, this inversion had high sensitivity (90%), specificity (100%), positive and negative predictive values (100% and 76.9% respectively), and accuracy (92.5 %) for the detection of hepatic steatosis (Lessa et al., 2010), which is compatible with the findings described in the literature (Biller et al., 1992; Palmentiere et al., 2006).

Rats with mild hepatic steatosis can appear to be normal in US examination (Lessa et al., 2010). The US has been reported to have sensitivity of 90-91% for the detection of moderate to marked steatosis, but its sensitivity decreases to 30–64% when fatty liver is mild (Biller et al., 1992; Palmentiere et al., 2006). In addition, it is important to exclude kidney diseases when using this approach (Biller et al., 1992).

The evaluation of portal hypertension is important to access the severity of the disease. One of its most important signs is the widening of the portal vein (Fig.7). The PVC presented statistically significant differences ($p<0.001$) between cirrhotic and non-cirrhotic rats. The increase in its caliber, which was greater or equal to 2.1mm, can be considered a relevant ultrasound parameter, with sensitivity of 100% and specificity of 90.5 % (Lessa et al., 2010). Additionally, a 50% increase in PVC after cirrhosis induction can be another good parameter for advanced hepatic fibrotic change (Mannheimer et al., 2009).

Among the imaging diagnostic methods, the ultrasound is considered ideal for the study of ascites, which can be observed even when mild. Considering diffuse hepatic disease, the presence of ascites invariably corresponds to cirrhosis (Fig. 8)

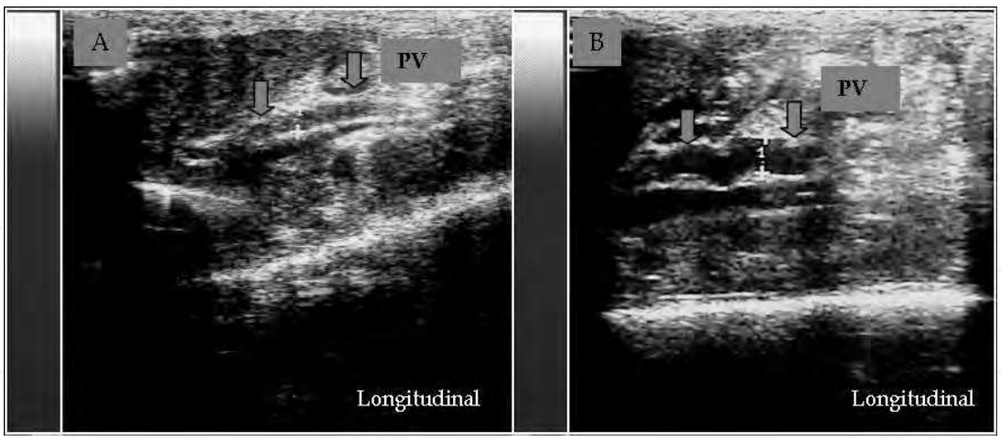

Fig. 7. Portal vein caliber (PVC): Longitudinal scans - [7A] Straight and thin portal vein (caliber=1.4 mm) in a healthy rat (arrows); [7B] Tortuous and dilated portal vein (caliber=2.2 mm) in a cirrhotic rat (arrows).

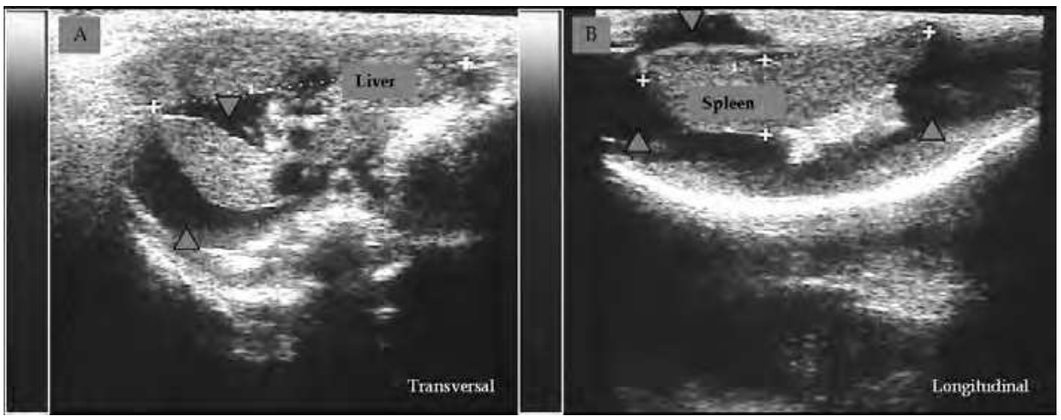

Fig. 8. [8A] Transversal liver sonogram shows a small cirrhotic liver with marked ascites; [8B] Longitudinal sonogram presents a great amount of ascites surrounding the spleen.

2.4 Focal liver lesions

Focal hepatic lesions are more easily detected by ultrasound when these lesions have a different echogenicity than the surrounding normal liver. Focal hepatic diseases include cysts, hematomas, abscess, granulomas, regenerative nodules, primary and metastatic neoplasms (Partington & Biller, 1995). US usually detects and characterize these lesions.

Regenerative hepatic nodules are benign reorganized masses of hepatic tissue that contain lipid, blood-filled sinusoids, lymphocytes and areas of atrophied or necrotic hepatocytes. These nodules are most commonly isoechoic and can be multiple and variably sized (Fig. 9).

Primary hepatic neoplasia may appear as solitary or multiple focal lesions that can be hypo, iso or hyperechoic in relation to normal liver. Also it can appear as a very large, moderately circumscribed or infiltrating mass. The US appearance of liver neoplasia is not specific for the histopathological cell type (Partington & Biller, 1995).

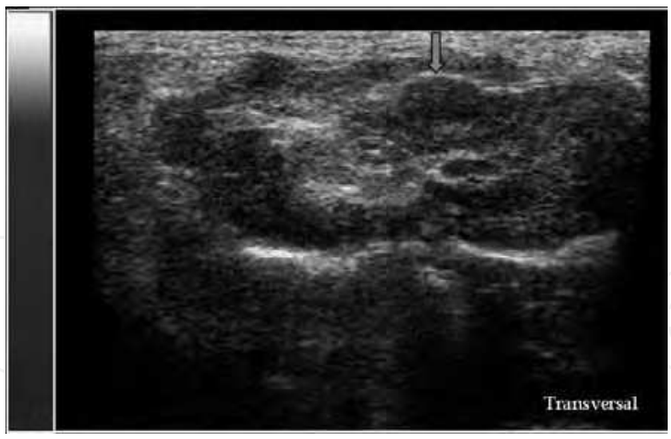

Fig. 9. Transversal sonogram shows a cirrhotic liver with an isoechoic regenerative nodule (arrow).

3. Human liver ultrasound imaging

The liver is the largest abdominal organ weighting 1.5 kg and lying in the right side of the upper abdomen under the right hemidiaphragm and extending across the midline to the left hypochondrium. The parenchymal echoes are a mid-grey and consist of a uniform, sponge-like pattern interrupted by the vessels. In transverse sections the wedge shape of the liver is seen, tapering to the left (Fig.10A). The caudate lobe is seen as an extension of the right lobe in transverse sections and as an almond-shaped structure posterior to the left lobe in longitudinal views (Fig.10B). In the longitudinal sections the liver has a triangular shape, the right lobe larger than the left (Fig. 10C).

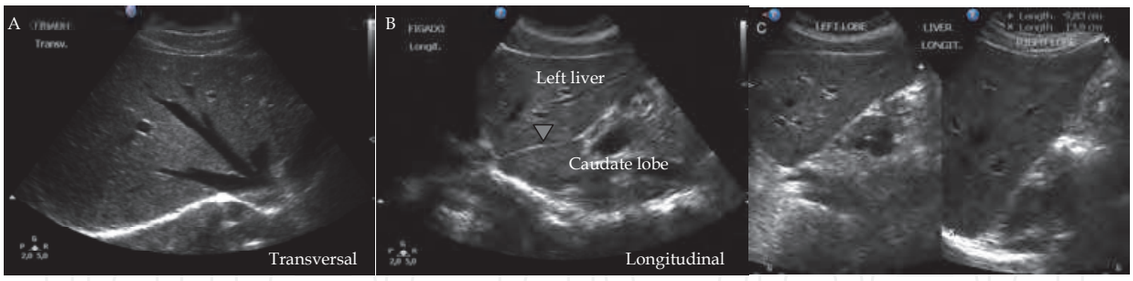

Fig. 10. [A] Transversal section of normal liver with the hepatic veins draining into the inferior vena cava. [B] Longitudinal scan of the left and caudate lobe being separated by the fissure of the ligamentum venosum (arrowhead); [C] Longitudinal scan of the liver: normal left lobe and right lobe.

3.1 Technique

The liver is best imaged with the patient supine or in a right anterior oblique position. Intercostal imaging is always required, in which case the transducer is placed parallel to the adjacent ribs to avoid acoustic shadowing. Multiplanar imaging of the liver is obtained. Sagittal, transverse, coronal and subcostal oblique views are required. A 5-2 MHz curved array transducer with appropriate gain and depth settings permits adequate visualization of the entire liver. A wide field of view in the near field is essential for good liver imaging. The

liver should be imaged in real-time in the sagittal and transverse or oblique planes. The left lobe is usually best imaged with the patient supine and the transducer placed in an anterior subxiphoid position. Real-time imaging during suspended deep inspiration allows the most superior aspects of the left lobe to be visualized. The right lobe usually requires an intercostal or subcostal oblique approach with the patient supine and in the left-side-down decubitus position. Certain regions are more difficult to image such as the high dome and the lateral aspect of the right lobe of the liver, usually best imaged from subcostal oblique and intercostal planes in suspended inspiration. The patient should be fasting for at least 6 hours prior to the exam to limit bowel gas and so that the gallbladder is not contracted.

3.2 Focal liver lesions

Liver masses are increasingly being identified due to the widespread use of imaging modalities. The majority of these lesions are detected incidentally in asymptomatic patients. Characterization of a liver mass on sonography is based on the appearance of the mass on gray scale imaging as well as on vascular information that may be obtained on Doppler examination.

3.2.1 Hepatic cysts

Simple cysts are usually described as congenital lesions, but are probably better considered developmental, since their frequency increases with age. Simple hepatic cysts are usually solitary, have a thin epithelial lining, and contain watery fluid. Their size varies from less than 1 cm to more than 20 cm in diameter. Simple cysts are found 4 times more frequently in females than males. Symptoms are rare, but may occur from mass effect, rupture, hemorrhage or infection. The classic sonographic findings are well known: a well defined, anechoic lesion with a well-demarcated, thin wall and good distal sonic enhancement (Fig. 11A). Thin septations are frequent, and should not suggest a different diagnosis. Occasionally there may occur cyst hemorrhage or infection when it will contain internal echoes and septations, a thickened wall and may appear solid (Fig. 11B). If thick septae or nodules are seen, differential diagnosis of biliary cystadenomas and cystic metastases must be considered. Acquired cysts are usually secondary to trauma, inflammation or parasitic infection and are indistinguishable from primary cysts. Cyst ablation with alcohol or surgical excision can be performed if indicated.

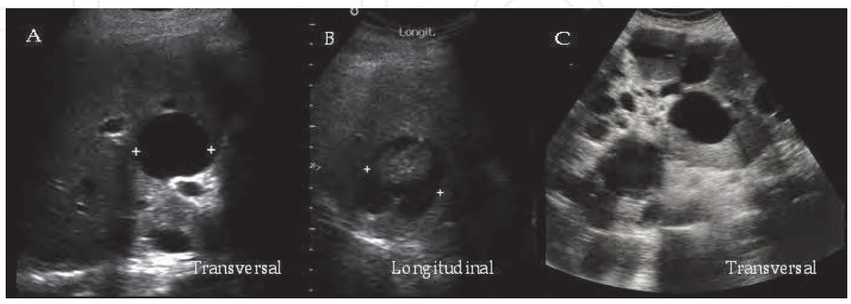

Fig. 11. [A] Hepatic cyst: a well defined, anechoic lesion with a thin wall and good distal enhancement; [B] Hemorrhagic cyst - a well defined cystic lesion with internal amorphous echoes and septation; [C] Polycystic liver disease: multiple anechoic cysts of varying sizes, thin walls and posterior distal enhancement. Note that some cysts contain internal echoes with fluid/fluid level due to internal hemorrhage.

Polycystic renal disease is a relatively common congenital condition and has an autosomal dominant mode of inheritance. Liver cysts are associated with this condition in approximately 57% to 74% (Levine et al., 1985). The most common presentation is hepatomegaly. The ultrasound appearance of multiple cysts of varying sizes, thin walls and posterior acoustic accentuation is characteristic (Fig. 11C). Hemorrhage or infection in the cysts may produce internal echoes. Acoustic accentuation beyond each cyst may produce the impression of an abnormal liver parenchymal texture. There may be cysts in other organs like pancreas, spleen, ovaries and lungs. Usually they do not require any treatment and complications are rare including hemorrhage, rupture or infection.

3.2.2 Biliary hamartomas (von Meyenburg Complexes)

Bile duct hamartomas are small focal developmental lesions composed of groups of dilated intrahepatic bile ducts with a collagenous stroma. They are benign liver malformations that are detected incidentally in 0.6 to 5.6% of reported autopsy series (Redston & Wanless, 1996). Commonly they are documented on sonograms as bright echogenic foci with distal ringdown or comet tail artifacts, diffusely distributed until the periphery of the liver (Fig. 12A-B) that could be related to the presence of tiny cysts beyond the resolution of the ultrasound equipment or to the cholesterol crystals within the dilated tubules. They may also appear as well-defined small hypoechoic solid nodules (Fig. 12C-D).

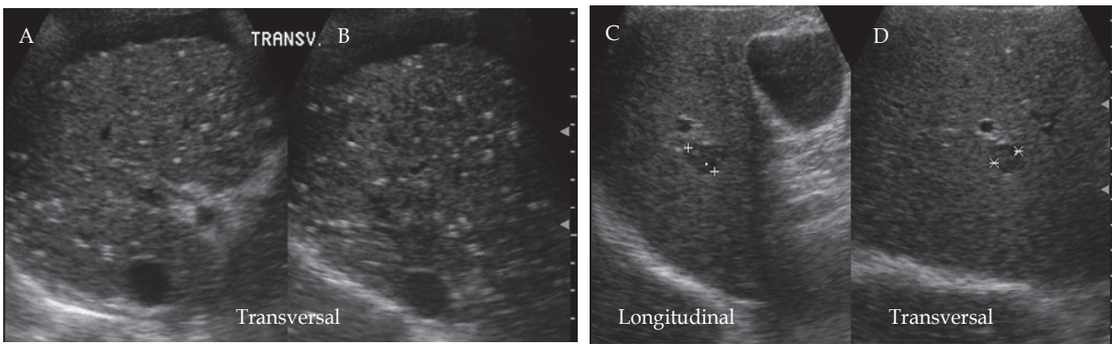

Fig. 12. Biliary hamartomas: [A-B] multiple bright echogenic foci some of them with distal ringdown or comet tail artifacts, diffusely distributed until the periphery of the liver; [C-D] Small hypoechoic nodule that on MRI was confirmed to be von Meyenburg complex.

3.2.3 Hydatid disease

The liver is the most frequently involved organ in hydatid disease but other sites may be involved, such as the lungs, the bones, the brain and the peritoneal cavity. In the liver the right lobe is more frequently involved where they form slow-growing cysts. Lewall & McCorkell (1985) proposed four groups of sonographic features of hepatic hydatid disease: solitary cysts containing sand; cysts with detached endocyst secondary to rupture; cysts with daughter cysts; and densely calcified masses. The distinction between simple and hydatid cysts may be one of the following features: wall calcification, debris consisting of sand and the two layers of the wall resulted from detachment and collapse of the inner germinal layer from the exocyst. The development of daughter cysts produces a characteristic appearance.

3.2.4 Hepatic abscess

Liver abscesses are frequently related to direct extension from the biliary tract infection in patients with suppurative cholangitis and cholecystitis or to complications of an intra-abdominal infection with direct portal venous system spread to the liver, such as diverticulitis or appendicitis. They may also be present in the liver as a result of blunt or penetrating trauma or through the hepatic artery in patients with osteomyelitis and subacute bacterial endocarditis. No cause can be found in approximately 50% of the cases of hepatic abscesses (Wilson & Withers, 2005).

Sonographically, pyogenic liver abscess has a variable appearance. Typically, pyogenic abscesses are poorly defined, irregularly marginated, and primarily hypoechoic. Irregular areas of increased echogenicity are frequent (Fig.13A-B). Bright punctate echoes often represent gas within the abscess. On occasion, a diffusely hyperechoic appearance may be noted, related to large amounts of gas from gas-forming organisms (Fig. 13C-D). Fluid-fluid interfaces, internal septations and debris can be observed. The abscess wall can vary from well-defined to irregular and thick. Diffuse microabscesses may occasionally cause a confusing sonographic pattern of increased irregular hepatic echogenicity. The differential diagnosis of pyogenic liver abscess includes complicated hepatic cysts with hemorrhage, hematoma, amebic infection and necrotic neoplasm.

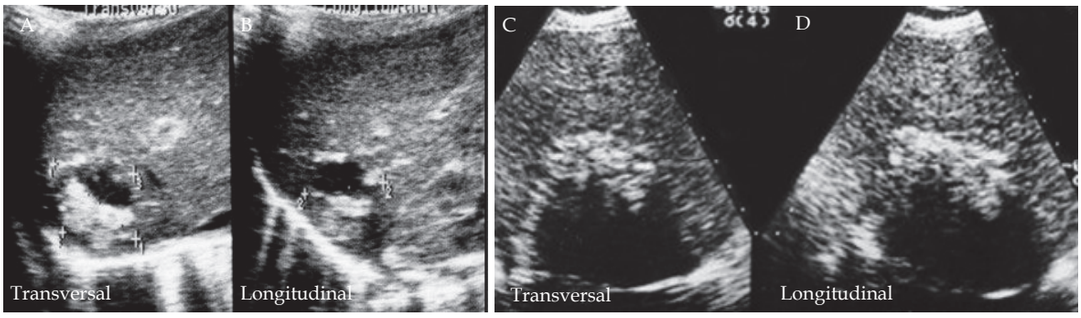

Fig. 13. [A-B] Hepatic abscess - Thick wall fluid collection with hyperechoic heterogeneous internal echoes; [C-D] Gas forming abscess - diffusely irregular hyperechoic lesion with posterior accoustic attenuation.

Entamoeba histolytica primarily infects the colon. Transmission is by the fecal-oral route. Amebic liver abscess is the most common non-enteric complication of amebiasis. The most common presenting symptom is pain. An amebic abscess may be indistinguishable from a pyogenic abscess. Sonographic features include lack of a significant wall echo, symmetric oval or round configuration, hypoechogenicity compared to normal liver with a homogeneous pattern of internal echoes, increased sound transmission and subcapsular location (Fig. 14). Ralls et al. (1987a) in a review of 112 amebic lesions described two sonographic patterns that were more prevalent in amebic abscesses: round or oval shapes in 82% versus 60% of pyogenic abscess and hypoechoic appearance with fine internal echoes at high gain in 58% versus 36% of pyogenic abscesses. The majority of hepatic amebic abscesses disappear with amebicidal drugs (Ralls et al., 1987b).

3.2.5 Cavernous hemangioma

Cavernous hemangiomas are the most frequently encountered benign tumor of the liver and are seen in 1 to 4% of the population as an incidental finding. These lesions are most

Fig. 14. Amebic abscess: lack of significant wall echo, round hypoechoic liver lesion with increased sound transmission and subcapsular location.

commonly seen in women with a female/male ratio of 5:1 (Snover, 2009). Hemangiomas are composed of dilated endothelial-lined vascular channels, infiltrated by varying degrees of fibrous stroma.

The typical hemangioma is a uniformly well circumscribed hyperechoic mass less than 3 cm in diameter. These lesions are often small and can be multiple (Fig. 15A-B). The increased echogenicity has been related to the numerous interfaces between the walls of the cavernous sinuses and the blood within them. In the setting of hepatic steatosis or cirrhosis, however, they may appear hypoechoic. Although this lesion is hyperechoic, in many cases hemangiomas will exhibit posterior acoustic enhancement because the dilated, fluid-filled sacs of blood do not attenuate sound. An atypical but not uncommon sonographic appearance of the hemangioma is a lesion with an echogenic rim and an internal hypoechoic pattern (Wilson & Withers, 2005) (Fig.15C-D). Larger lesions tend to be heterogeneous with central hypoechoic foci corresponding to fibrous collagen scars, large vascular spaces, or both. Calcification is rare. Hemangiomas only rarely demonstrate internal flow on Doppler studies, due to the multidirectionality and slow velocity of flow. There are potentially significant lesions that may mimic the morphology of a hemangioma on ultrasound and produce a single mass or multiple masses of uniform increased echogenicity such as metastases from a colon primary tumor; small hepatocellular carcinomas (HCC) may show this morphology. Caturelli et al. (2001) in a prospective evaluation of 1982 patients with newly diagnosed cirrhosis found that 50% of echogenic liver lesions suggestive of

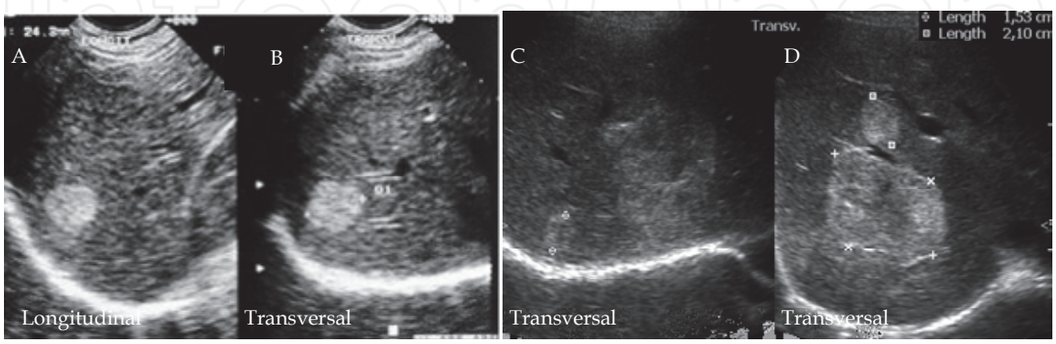

Fig. 15. Hemangioma: [A-B] Typical hemangioma: hyperechoic round lesion at the posterior segment of the right lobe of the liver with posterior acoustic enhancement; [C-D] Multiple hemangiomas: Multiple echogenic lesions with central hypoechoic areas.

hemangiomas had the diagnosis of HCC. These results emphasize the importance to prove the diagnosis of all masses with this morphology in high-risk patients.

3.2.6 Focal nodular hyperplasia

Focal nodular hyperplasia (FNH) is the second most commonly encountered benign liver lesion and is seen most often as an incidental observation in a young adult female. FNH is not an actual neoplastic tumor but represents instead a hyperplastic response to an underlying vascular malformation in the liver. Histologically, it is made up of normal liver components, including hepatocytes and Kupffer cells. FNH is a hypervascular lesion, often showing a central stellate vascularity and a large and tortuous feeding artery. On sonography, FNH is often a subtle liver mass that is difficult to differentiate in echogenicity from the adjacent liver parenchyma (Fig.16A-B). The lesions may be slightly hypoechoic, isoechoic, or slightly hyperechoic than the surrounding liver. Use of color and power Doppler US may add information concerning the vascularity of the suspected FNH. In addition, use of US contrast media to characterize FNH has been reported. These lesions usually produce a contour abnormality to the surface of the liver or may displace the normal blood vessels within the parenchyma. The central scar may be seen on gray-scale sonograms as a hypoechoic linear or stellate areas within the central portion of the mass. Well-developed peripheral and central blood vessels are seen to course within the central scar with either a linear or stellate configuration (Fig.16C-D). Spectral interrogation usually shows predominantly arterial signals centrally.

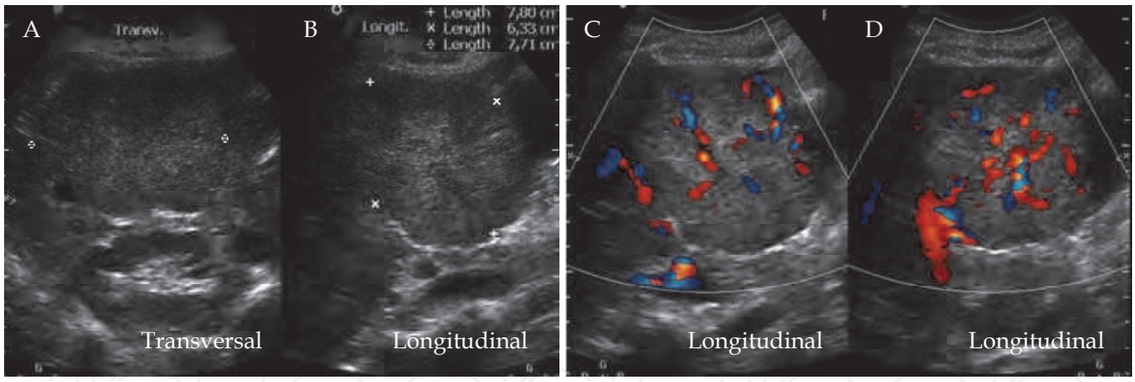

Fig. 16. Focal Nodular Hyperplasia. [A-B] Isoechoic large lesion in the right lobe deforming the contour of the liver with a subtle hypoechoic central area; [C-D] Color Doppler showing stellate pattern blood vessels within the central scar.

3.2.7 Hepatic adenoma

Hepatic adenomas (HA) are less common than FNH, benign neoplasms, usually solitary and well encapsulated, ranging in size from 8 to 15 cm, which have a small risk for malignant transformation into hepatocellular carcinoma, as well as a propensity for hemorrhage and rupture. The majority of these lesions occur in young women taking oral contraceptives. The risk of developing HAs is related to both the duration of use and dose of hormones. These lesions regress when oral contraceptives are discontinued (Fig.17A-F). Other populations noted to have an increased incidence of HAs include individuals with type I glycogen storage disease. In these patients, hepatic adenomas tend to be multiple. The sonographic

appearance is nonspecific. Although in 70% to 80% of cases, HAs present as a solitary and large hyperechoic lesion with central anechoic areas, corresponding to zones of internal hemorrhage, they can be isoechoic or complex masses. It is difficult to distinguish hepatic adenoma from FNH. Color Doppler evaluation can be helpful, demonstrating peripheral and intratumoral vessels showing increased venous structures within the center of the mass and a paucity of arterial vessels (Fig.17G-H). These lesions are substantially less vascular than most FNH (Wilson & Withers, 2005).

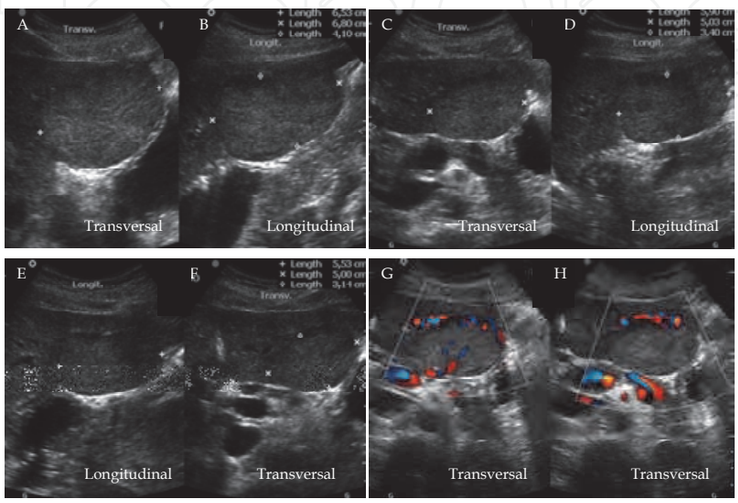

Fig. 17. Hepatic Adenoma: [A-F] Isoechoic lesion in the left lobe of the liver that diminished in size as oral contraceptives were discontinued (A-B: 1st exam, C-D: 2nd exam, E-F: 3rd exam-every two months); [G-H] Color Doppler showing predominantly peripheral vessels.

3.2.8 Hepatocellular carcinoma

Hepatocellular carcinoma (HCC) is the commonest primary liver cancer, comprising 80% of primary liver malignancies in the United States. The majority of HCC patients (95% in the western, 60% in Asian countries) will develop the disease on the ground of preexisting liver cirrhosis. Alcoholic cirrhosis-related HCC has a lower frequency (10% of autopsied patients) than HBV or HCV (Parkin et al., 2005). Although α-fetoprotein (AFP) is a known and specific tumor maker for HCC, it is not suitable for the screening and surveillance of HCC because of its poor predictive value and low sensitivity. The use of imaging modalities is essential for the screening, diagnosis and treatment of HCC. US plays a major role among them, because it provides real-time and noninvasive observation by a simple and easy technique. The development of digital technology has led to the detection of blood flow by color Doppler US, and the sensitivity for detecting tumor vascularity has shown remarkable improvement with the introduction of microbubble contrast agents. Screening generally consists of serologic testing for alpha-fetoprotein and/or hepatitis B and C, often coupled with sonography of the liver. Some studies showed that surveillance based on US and AFP every 6-12 months improved the survival of patients (Bolondi et al., 2001; Sangiovanni et al., 2004). Pathologically HCC occurs in three forms: 1. Solitary tumor; 2. Multiples nodules; 3. Diffuse infiltration. Sonographic findings in HCC are variable, and may cause difficulty in distinguishing advanced HCC from metastatic disease. This is less of a problem in screening programs, where HCCs less than 5 cm are often detected. In these small lesions, sonographic

findings are not as diverse. About 75% of small HCCs (<5 cm) are hypoechoic (Fig.18A-B). As HCCs enlarge, they tend to develop hypoechoic peripheral rims. With further progression, lesions become more numerous and heterogeneous. Some hepatocellular carcinomas, even small lesions, undergo fatty metamorphosis, causing increased echogenicity and potential confusion with hemangioma. Hepatocellular carcinomas arising in normal livers are uncommon. Fibrolamellar HCC, which accounts for 2% of hepatocellular carcinoma, but 25% to 50% of HCC in young adults, often arises as a single well-circumscribed lesion with lobulated margins in an otherwise normal liver. Other features may include a "central scar" and a high prevalence of calcification. Vascular invasion is common and should suggest the diagnosis of HCC. HCC invades portal veins more frequently than hepatic veins. Intravascular tumor is usually reflective and expands the vessel, but positive differentiation from blood thrombus depends on detecting arterial Doppler signals from within the thrombus (Fig. 18C-F); only venous signals are found in blood thrombus as it is recanalized. HCC has a characteristic hypervascular appearance with centripetal blood flow, and a basket pattern is one of the typical findings of HCC by color Doppler imaging (Tanaka et al., 1990). Using microbubble contrast agents HCC shows as a highly vascular lesion in the overwhelming majority of patients studied.

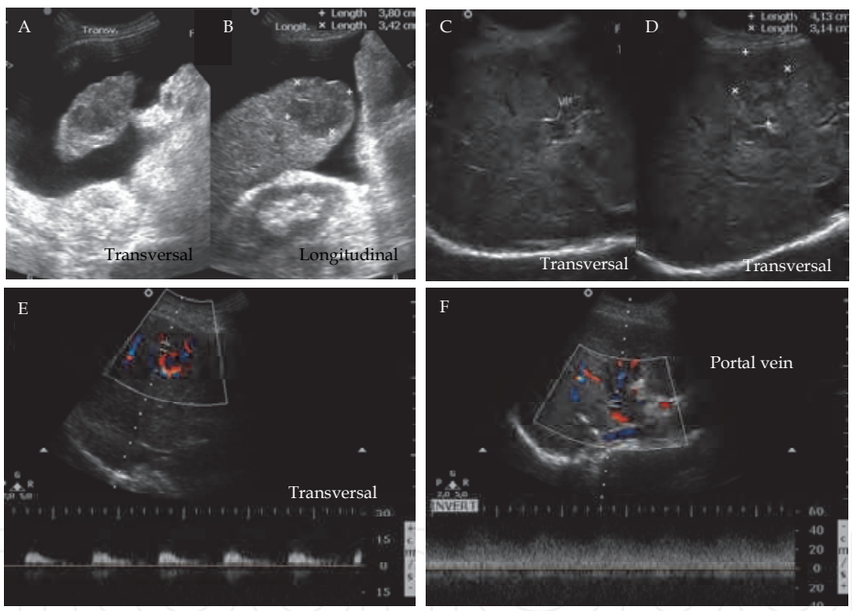

Fig. 18. Hepatocellular Carcinoma: [A-B] Lobulated hypoechoic lesion in the periphery of the right lobe; [C-F] Hipoechoic lesion in segment IV with portal tumoral thrombus. Note on color Doppler that the lesion has intra and peripheral vascularity (E) and that there is arterial flow inside the portal vein (F).

3.2.9 Cholangiocarcinoma

Cholangiocarcinoma arises from the bile ducts, and account for about 10% of all primary liver cancers. Cholangiocarcinoma is associated with hemochromatosis, ulcerative colitis, Caroli disease and choledochal cyst. Cholangiocarcinoma has two forms, peripheral cholangiocarcinoma (PCC) and hilar cholangiocarcinoma, also known as Klatskin tumor, when it involves the confluence of the left and right hepatic ducts at the porta hepatis. In the

United States, PCC is 3 times more common than hilar cholangiocarcinoma. The prevalence is equal in Japan. PCC is usually a large tumor, while hilar cholangiocarcinoma presents earlier with ductal obstruction and jaundice, and is usually not associated with a large mass. Hemochromatosis is associated with both PCC (9% of patients) and HCC (18% of patients). The sonographic findings in PCC are variable. In general, cholangiocarcinomas are hard to visualize with all modalities. Some investigators report predominance of hypoechoic lesions, and others predominantly hyperechoic lesions. Our experience suggests that slightly hypoechoic lesions are more frequent. Portal venous invasion is frequent. Sonography is generally superior to multiphase helical CT in demonstrating masses associated with hilar cholangiocarcinomas. Dilatation of the biliary tree can be followed down to the point of obstruction, where it may be possible to detect a solid, poorly reflective mass which, if large enough, can be seen to have a heterogeneous internal echo pattern and ill-defined margins (Fig.19).

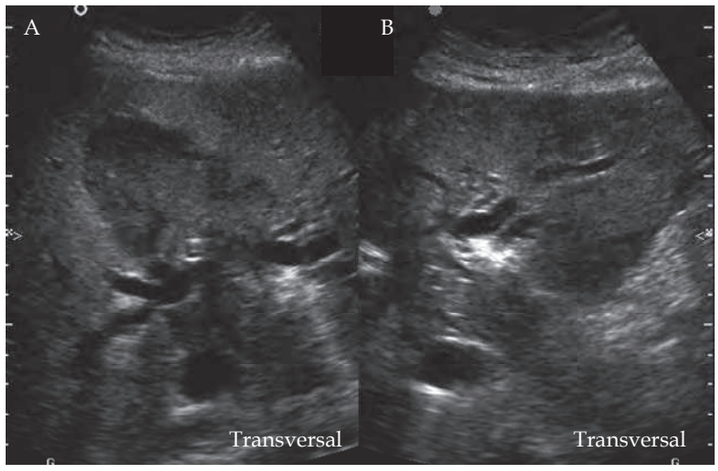

Fig. 19. Cholangiocarcinoma: large hilar hypoechoic mass with right and left intrahepatic bile ducts dilatation.

3.2.10 Metastatic disease

In the United States, metastatic disease is by far the most common significant focal liver lesion. Metastases are 18 to 20 times more common than hepatocellular carcinoma (HCC) and produce symptoms 10 times more frequently. In one large autopsy series (Edmonson, 1987), 38% of all patients with carcinoma had hepatic metastases. The most common carcinomas metastasizing to the liver include, in order of decreasing frequency: gallbladder, colon, stomach, pancreas, breast and lung. Metastatic disease is multifocal in approximately 90% of patients. Most metastases to the liver are blood-borne via the hepatic artery or portal vein. The portal vein provides direct access to the liver for tumor cells originating from the gastrointestinal tract and probably accounts for the high frequency of liver metastases from organs that drain into the portal circulation. Virtually any sonographic appearance may occur in liver metastasis. The following sonographic appearances of metastatic liver disease have been described: echogenic, hypoechoic, target, calcified, cystic and diffuse. Hypoechoic halos are common. The presence of a hypoechoic halo surrounding a liver mass has been regarded as an ominous sign with a high association with malignancy, particularly metastatic disease. Wernecke et al. (1992) described the importance of the hypoechoic halo in the differentiation of

malignant from benign focal hepatic lesions. Its identification has a positive and negative predictive value of 86% and 88%, respectively. Echogenic metastases tend to arise from a gastrointestinal origin or from HCC (Fig.20A). While it must be emphasized that sonographic appearance is a poor predictor of the primary tumor, certain patterns may be suggestive. For example, large to moderate-sized hyperechoic metastases, especially those with microcalcifications, should suggest the possibility of a colonic primary. A target or bull's eye appearance with varying rings of hypo- and hyperechogenicity are common (Fig. 20B). Ill-defined infiltrative disease with focal nodularity is another fairly frequent pattern. Metastasis and HCC may be impossible to distinguish sonographically, although the presence of underlying liver disease favors HCC. Invasion of the portal or hepatic veins suggests hepatocellular carcinoma, rather than metastasis. Most liver metastases that are hypoechoic are hypovascular. Colon, lung, breast, and gastric cancers are the most common causes of hypovascular liver metastases (Fig.20C). The most common causes of hypervascular hepatic metastases include neuroendocrine tumors (eg, carcinoid, pheochromocytoma, and islet cell tumors), renal cell carcinoma, melanoma, choriocarcinoma, and thyroid carcinoma. Breast carcinoma and, rarely, pancreatic adenocarcinoma can also cause hypervascular metastases.

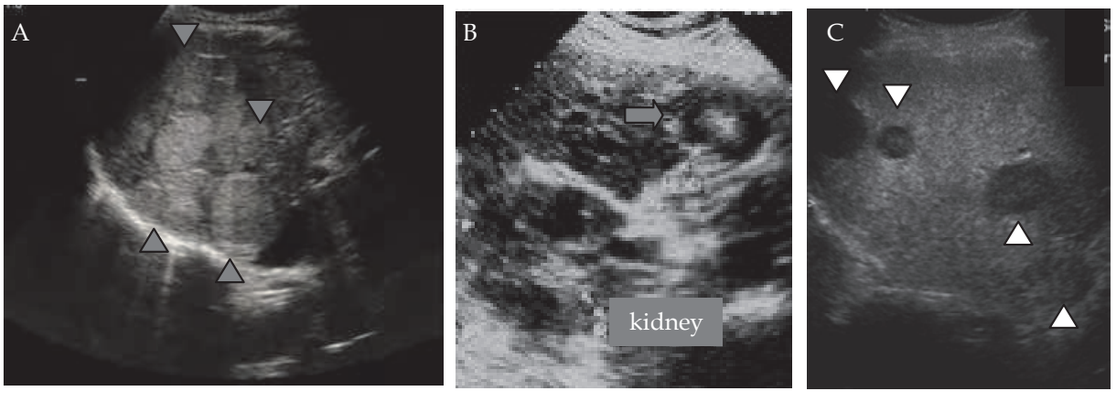

Fig. 20. Metastases: [A] Multiple echogenic nodular lesions due to HCC metastases (gray arrowheads); [B] Bull's eye appearance and another echogenic lesion secondary to colon carcinoma (arrow); [C] Multiple hypoechoic nodular lesions; metastases from cholangiocarcinoma (white arrowheads).

3.3 Diffuse liver disease

Recent innovations in imaging technology and contrast media development have augmented the role of radiology in the detection, characterization, and follow up of diffuse liver diseases. Although biopsy still remains the gold standard for establishing the diagnosis of diffuse liver disease, imaging is used to narrow the differential diagnosis, to follow up patients in which the diagnosis has been made, to detect complications, and to monitor response to therapy.

3.3.1 Fatty liver

Hepatic steatosis or fatty changes is an acquired, reversible disorder of metabolism and can result from a variety of pathologic processes including increased production or mobilization of fatty acids (e.g., hyperalimentation, starvation, obesity, steroid use, diabetes mellitus, and gastrointestinal bypass surgery) or decreased hepatic clearance of fatty acids from

hepatocellular injury (e.g., alcoholic liver disease, hepatitis, drug-induced liver disease, and liver transplantation). The distribution of steatosis can be quite variable, ranging from focal to regional to diffuse. Histopathologically, the hallmark of all forms of fatty liver is the accumulation of fat globules within the hepatocytes. If accompanied by inflammation but not associated with alcohol abuse, the condition is called nonalcoholic steatohepatitis. Probably the most common cause of a fatty liver is obesity. Correction of the primary abnormality will usually reverse the process, although it is now recognized that fatty infiltration of the liver is the precursor for significant chronic disease in a percentage of patients.

Diffuse steatosis is common. It has been detected in up to 7% of abdominal CT examinations, and a relatively recent autopsy series found significant steatotic changes in 7% of nonobese patients and 29% of obese patients (El-Hassan et al., 1992; Wanless & Lentz, 1990). Generally, patients with steatosis are asymptomatic, although some individuals may present with abnormal liver function tests or right upper quadrant pain, the latter probably due to distention of Glisson's liver capsule from hepatomegaly. In patients with pure hepatic steatosis without coexistent hepatocytic injury, weight reduction or stopping the underlying etiologic factor usually reduces the amount of fatty change.

Sonography of fatty infiltration may be varied. Mild steatosis is detected when there is minimal diffuse increase in hepatic echogenicity with normal visualization of diaphragm and intrahepatic vessels (Fig.21A). Moderate steatosis is seen as moderate increase in hepatic echogenicity with slightly impaired visualization of intrahepatic vessels and diaphragm (Fig.21B). Severe steatosis is diagnosed when there is marked increase in echogenicity with poor penetration of the posterior segment of the right lobe of the liver and poor or nonvisualization of hepatic vessels and diaphragm (Fig.21C-D), the so-called bright liver on ultrasound (Taylor et al., 1986). Significant findings include hepatomegaly, decreased sonographic visualization of portal and hepatic veins and an unusual "fine" liver texture (Zwibel, 1995;).

Fig. 21. Diffuse steatosis: [A] Mild steatosis: minimal diffuse increase in hepatic echogenicity with normal visualization of diaphragm and intrahepatic vessels; [B]Moderate steatosis: moderate increase in hepatic echogenicity with slightly impaired visualization of intrahepatic vessels and diaphragm; [C-D] Severe steatosis: marked increase in hepatic echogenicity with nonvisualization of hepatic vessels and diaphragm.

3.3.2 Focal steatosis and focal sparing

Hepatic fatty change is not always uniform but can present as a focal or regional area of steatosis in an otherwise normal liver (focal steatosis) or as subtotal fatty change with sparing of certain areas (focal sparing) (Baker et al., 1985). Both processes are common and may cause considerable diagnostic confusion, especially in the workout of primary or metastatic malignant liver disease (Baker et al., 1985). Aberrant blood supply to those areas has been demonstrated to be the underlying etiology for nonuniform change (Arai et al., 1988). In

individuals with focal fatty sparing, it is assumed that the spared regions do not have a normal portal blood supply and therefore do not receive lipid-rich blood from the gut. Because of their underlying vascular aberrance, most of these spared areas have a characteristic location. For example, focal fatty sparing of the medial segment of the left liver lobe results from blood supply through the gastric veins, whereas aberrant blood supply from the internal thoracic artery has been established in some lesions around the falciform ligament (Matsui et al., 1995). Other characteristic locations include areas adjacent to the gallbladder fossa, the subcapsular region, and the porta hepatis. Islands of normal liver parenchyma may appear as hypoechoic masses within a dense, fatty infiltrated liver (Fig.22).

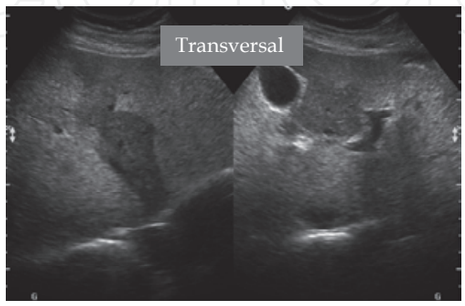

Fig. 22. Multifocal steatosis: multifocal increase in echogenicity of the liver parenchyma, sparing the segment IV that appears hypoechoic.

Less clear is why the same areas that can present as focal fatty sparing also have focal fatty infiltration. It is hypothesized that decreased delivery of unknown substances from the portal vein and relative ischemia from the paucity of portal blood supply are the main causative factors. In focal fatty infiltration, regions of increased echogenicity are present within a background of normal liver parenchyma and may present as a pseudonodular lesion (Fig.23). On imaging, several observational clues assist with correct identification of focal fatty change or focal spared areas:
1) typical periligamentous and periportal location,
2) lack of mass effect,
3) sharply angulated boundaries,
4) nonspherical shape,
5) absence of vascular displacement or distortion, and
6) lobar or segmental distribution.

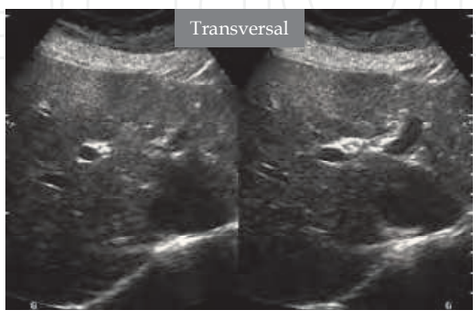

Fig. 23. Pseudonodular steatosis: Echogenic nodule (white arrow) in segment IVB anterior to the bifurcation of the portal vein that was confirmed to be a focal nodular steatosis in the MRI exam.

3.3.3 Cirrhosis

Cirrhosis is defined by the World Health Organization (WHO) as a diffuse process characterized by fibrosis and the conversion of normal liver architecture into structurally abnormal nodules. Liver cirrhosis is caused by diffuse fibrosis and regenerating nodules that result from liver cell necrosis and degeneration. It is characterized by architectural distortion and the development of a spectrum of nodules, ranging from benign regenerating nodules to HCC (Brown et al., 1997). In cirrhosis, in its early stages, the liver may appear normal. With progression of the disease, nodularity of the liver surface and generalized heterogeneity of the hepatic parenchyma can be seen. The porta hepatis and interlobar fissure frequently appear widened due to shrinkage of the right lobe and the medial segment of the left lobe, with concomitant enlargement of the caudate lobe and the lateral segment of the left lobe. The gross morphologic appearance of the cirrhotic liver is categorized by the size of the parenchymal nodules: micronodular, macronodular, or mixed. Micronodular cirrhosis is characterized by regenerative nodules of relatively uniform small size, ranging from 0.1 to 1.0 cm in diameter. This pattern is most commonly seen in chronic alcoholic cirrhosis. In macronodular cirrhosis, the parenchymal nodules are larger, coarser, and more variable in size, up to 5.0 cm in diameter. The most common cause of macronodular cirrhosis is chronic viral hepatitis.

The sonographic patterns associated with cirrhosis are:

1. Volume redistribution - In the early stages of cirrhosis, the liver may be enlarged, whereas in the advanced stages, the liver is often small, with relative enlargement of the caudate and the left lobe, and reduction of the size of the right lobe (Fig.24A). A ratio of caudate lobe to right lobe can be derived from a transverse scan of the liver immediately below the portal vein bifurcation: this is less than 0.6 in normal subject and greater than 0.65 in cirrhosis, with 100% specificity but sensitivities of 84% and 43% in two different series (Giorgio et al., 1986; Harbin et al., 1980);
2. Coarse echotexture - Increased echogenicity and coarse echotexture are frequent observations in diffuse liver disease (Fig.24B);
3. Nodular surface - Irregularity of the liver surface (Fig.24C);
4. Regenerative and dysplastic nodules - Regenerative nodules tend to be isoechoic or hypoechoic with a thin echogenic border. They may give a generalized granularity to the liver echotexture in forms of micronodular cirrhosis (Fig.24D). The larger nodules of macronodular disease may give an ultrasonically recognizable surface nodularity. Dysplastic nodules are considered premalignant.

Other ultrasound findings in cirrhosis are related to the complications associated with hepatocellular failure and portal hypertension: these include ascites, splenomegaly, the development of collateral venous channels and other abnormalities of the portal venous system.

3.4 Portal hypertension

Portal hypertension develops when increased resistance to portal flow and/or increased portal blood flow occur. Normal portal vein pressure is 5 to 10 mm Hg (14cm H2O). Portal hypertension is defined by a wedged hepatic vein pressure or direct portal vein pressure of more than 5 mm Hg greater than inferior vena cava pressure, splenic vein pressure of greater than 15 mm Hg, or portal vein pressure of greater than 30 cm H2O. They result in enlargement of the extrahepatic portal vessels, the development of spontaneous portosystemic collaterals and slow portal vein flow. Portal hypertension can be classified in

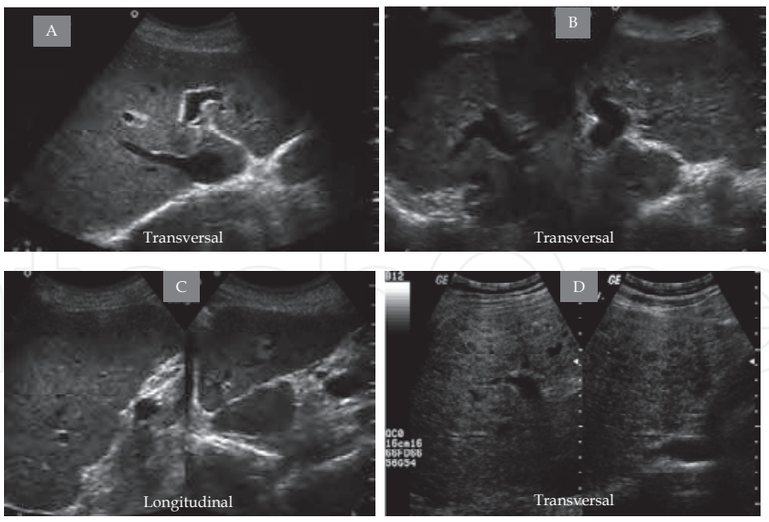

Fig. 24. Cirrhosis: [A] Volume redistribution with enlargement of the left and caudate lobes; [B] Volume redistribution with coarse echotexture; [C] Longitudinal scans showing lobulated contour; [D] Multiple small hypoechoic nodules along the entire liver parenchyma (regenerative).

several ways. We find that the easiest method is to divide it into intrahepatic, extrahepatic, and hyperdynamic. Extrahepatic portal hypertension can be subdivided into prehepatic (portal vein thrombosis, compression, and stenosis) and posthepatic (hepatic vein or inferior vena cava [IVC] thrombosis, compression, or stenosis). The extrahepatic presinusoidal portal hypertension should be suspected in any patient who presents with clinical signs of portal hypertension - ascites, splenomegaly and varices - and a normal liver biopsy. Thrombosis of the portal venous system occurs in children secondary to umbilical vein catheterization, omphalitis and neonatal sepsis. In adults, the causes of portal vein thrombosis include trauma, sepsis, HCC, pancreatic carcinoma, pancreatitis, portacaval shunts, splenomegaly and hypercoagulable states. Hyperdynamic refers to conditions that cause arterial portal fistulas or arteriovenous malformations. Extrahepatic portal hypertension and hyperdynamic portal hypertension are much less common than the intrahepatic category. Intrahepatic portal hypertension is subdivided into presinusoidal and postsinusoidal. The intrahepatic presinusoidal causes of portal hypertension include hepatic fibrosis, sarcoidosis, schistosomiasis, and lymphoma. Postsinusoidal includes cirrhosis and venoocclusive disease (Ralls, 1990).

Cirrhosis is the most common cause of intrahepatic portal hypertension. It causes hepatocellular death and parenchymal degeneration and regeneration. This results in bridging fibrosis that affects the central venules that drain the sinusoids, as well as the sinusoids themselves. The fibrosis causes increased resistance to blood flow. Initially, portal vein flow volume is maintained, but at a higher portal pressure. As the process progresses, the resistance to inflow in the liver equalizes with resistance to flow in portosystemic collaterals. At this point, portal flow starts to be diverted into the collaterals. As portal inflow to the liver decreases, hepatic arterial flow increases, and the arteries become larger and more tortuous. Eventually, resistance to arterial inflow reaches a point where arterial flow starts to shunt into the portal vein system. This initially produces portal vein flow reversal in isolated peripheral portal vein branches. But as more and more peripheral

branches reverse, flow in the major branches and eventually the main portal vein reverses (Ralls, 1990).

There are several sonographic findings of portal hypertension. Dilatations of the portal, mesenteric and splenic veins are all potential indicators of elevated pressures. Weinreb (1982) found 13 mm as the cutoff for upper limit of normal portal vein diameter. In general, an unusually large portal vein is a good sign of portal hypertension, but a normal size portal vein certainly does not exclude the diagnosis. Lack of caliber variation of the splenic and mesenteric vein during respiration is another parameter that has been investigated. This approach had a sensitivity of 80% and specificity of 100% in diagnosing portal hypertension (Bolondi et al., 1982).

A variety of Doppler techniques have been used to evaluate patients with suspected portal hypertension. Simple measurements of portal vein velocity are one such approach. Zirone et al. (1992) found a sensitivity of 88% and a specificity of 96% using a mean portal vein velocity cutoff of 15 cm/sec. Although there is general agreement that portal vein velocities usually decrease with portal hypertension, the expected values in control subjects and cirrhotic patients vary considerably. Mean portal venous flow velocity is approximately 15 to 18 cm/sec. Sources of variability include interobserver variability, intermachine variability, presence of variable collateral pathways (especially recanalized umbilical veins), and variations caused by differences in patient positioning, different phases of respiration, states of fasting, exercise status and cardiac output. These variations probably also account for the fact that portal velocities tend to decrease as portal pressures increase, but the correlation is not statistically significant (Choi et al., 2003; Haag et al., 1999). As portal hypertension develops, the flow in the portal vein loses its ondulatory pattern and becomes monophasic (Fig.25A-B). As the severity of portal hypertension increases, flow becomes biphasic and finally hepatofugal (Fig.25C). The ratio of portal vein cross-sectional area and portal velocity has been called the congestion index and has also been used to diagnose portal hypertension. Moriyasu et al. (1986) described this index based on the assumption that portal vein cross-sectional area will increase and the portal velocity will decrease in the setting of portal hypertension, resulting in a quotient that increases dramatically. In this study, it was shown that the congestion index was 2.5 times higher in patients with cirrhosis and portal hypertension than in control subjects. Normal values were described to be up to 0.099 cm x sec. The sensitivity of congestion index measurements ranges from 67% to 95% (Haag et al., 1999; Moriyasu et al., 1986).

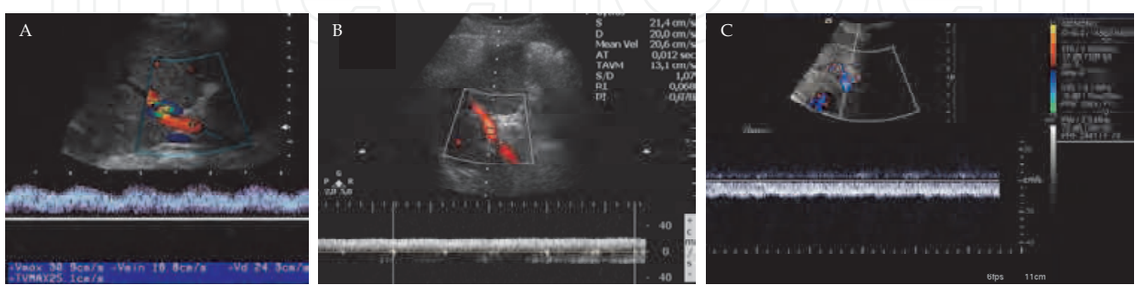

Fig. 25. Portal vein flow: [A] Ondulatory normal pattern; [B] Loss of ondulatory flow, mantaining the normal hepatopetal flow; [C]Hepatofugal portal vein flow as seen with the blue color inside the vein and the graphs below the baseline.

Alterations in the hepatic venous waveform can also occur with cirrhosis and portal hypertension. In general, the normal pulsatility of hepatic veins is either blunted or completely eliminated in patients with cirrhosis (Fig.26A-C). In fact, complete loss of any pulsatility has been shown to correlate with a higher Child-Pugh score and decreased survival rate (Ohta et al., 1995). The mechanism for this loss of hepatic vein pulsatility is unclear, but is likely related to hepatic vein loss of compliance due to hepatic fibrosis or stenosis, which can be caused by impression on the hepatic veins by regenerating nodules (Lorenz & Winsberg, 1996).

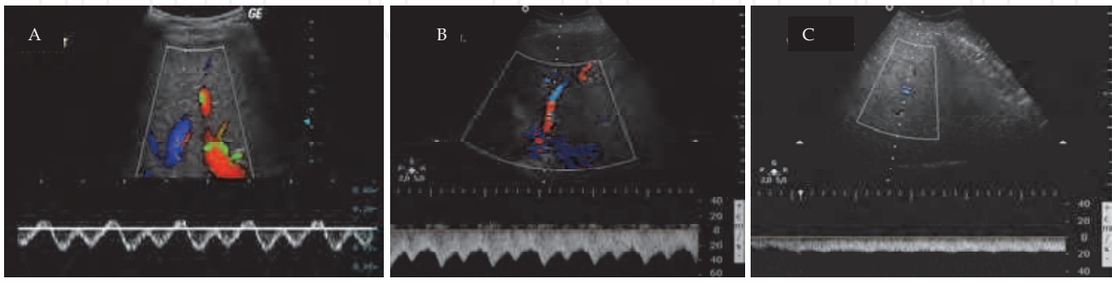

Fig. 26. Hepatic vein flow: [A] Normal triphasic flow; [B] Biphasic flow; [C] Monophasic (portalized) flow.

Although measurement of vessel diameters and velocities and calculation of various indices have shown promise in certain studies, the most reliable and widely used approach for the diagnosis of portal hypertension is the detection of portal systemic collaterals. The left gastric vein is the most prevalent portal systemic collateral present in 80% to 90% of patients with portal hypertension (Burcharth, 1979; Nunez et al., 1978) and its presence implies an increased risk for variceal hemorrhage. Sonographically, the left gastric vein is identified as a vessel communicating with the superior aspect of the portal or splenic vein in the region of the confluence (Fig. 27). The left lobe of the liver serves as an acoustic window, and when the left lobe is small, it may be difficult to visualize this vein. It extends superiorly and to the left and typically travels immediately anterior to the bifurcation of the celiac axis. The upper limit of normal for the vein diameter is 5 to 6 mm (Lafortune et al., 1984; Wachsberg & Simmons, 1994). Unfortunately, dilatation of the left gastric vein above a diameter of 6 mm occurs in only 25% of patients with portal hypertension, and it is not necessarily present for variceal hemorrhage to occur (Wachsberg & Simmons, 1994). On the other hand, the left gastric collateral was the only portal systemic collateral visualized in approximately 75% of patients. Other tributaries of the portal system can function as portal systemic collaterals and include short gastric veins and branches of the superior and inferior mesenteric veins. Identification of hepatofugal flow in any of these vessels is adequate to establish the diagnosis of portal hypertension.

Normally, the umbilical vein is an obliterated fibrous remnant that runs in the ligamentum teres. It can be identified in some patients as a hypoechoic band running within the fat of the ligamentum teres. It extends from the umbilicus to the most anterior aspect of the umbilical segment of the left portal vein. In individuals with no portal hypertension, no flow is present in the obliterated umbilical vein, and the fibrous remnant measures less than 3 mm (Gibson et al., 1989). In the setting of portal hypertension, the umbilical vein recanalizes and develops hepatofugal flow. The recanalized umbilical vein is best seen by scanning the left lobe of the liver and identifying the umbilical segment of the left portal vein. The umbilical

vein itself travels inferiorly from the umbilical segment of the left portal vein and exits the liver where it extends inferiorly along the abdominal wall to the umbilical area (Fig.28A-B). From there, it extends further inferiorly to communicate with the inferior epigastric veins. Ultimately, it communicates with the iliofemoral system and in this way diverts blood back to the systemic circulation. Although these 2 collaterals are the easiest and most productive to analyze, there are other collaterals that can be detected sonographically, albeit with more difficulty in some cases. These include short gastric, splenorenal, splenoretroperitoneal, superior mesenteric, and inferior mesenteric collaterals.

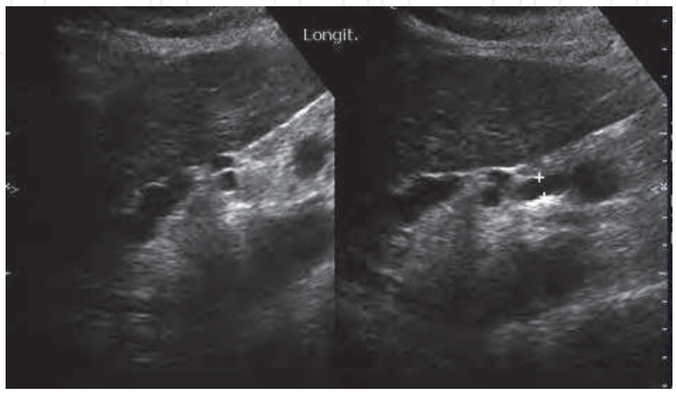

Fig. 27. Left gastric vein: Dilated left gastric vein in a longitudinal scan below the left lobe of the liver.

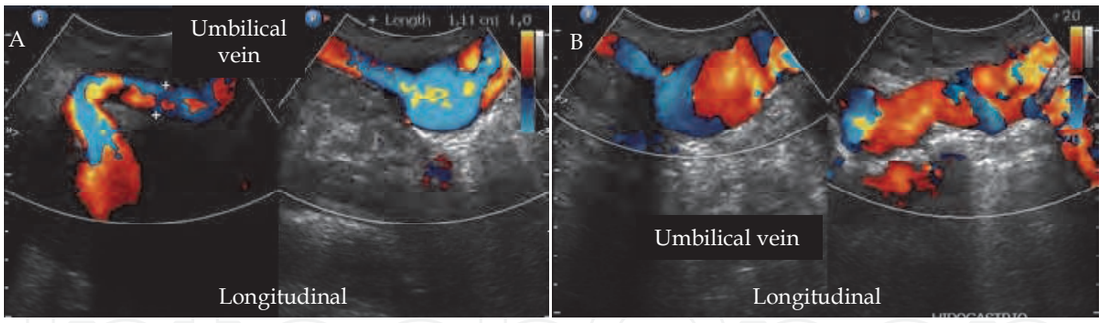

Fig. 28. Umbilical vein: [A-B] Recanalized umbilical vein from the falciform ligament to the anterior abdominal wall in the umbilical area going down to the hypogastrium.

Splenorenal collaterals are large spontaneous porto-systemic shunts from the splenic hilum or capsule to the left renal vein. It is often difficult to trace these collaterals from the splenic vein to the renal vein in continuity. Many times, the detection of multiple collaterals around the splenic hilum and an enlarged left renal vein is enough to make the presumptive diagnosis of a splenorenal collateral (Fig.29A-B). Splenoretroperitoneal collaterals may communicate with perivertebral vessels or gonadal vessels. Superior mesenteric collaterals communicate with pancreaticoduodenal veins and retroperitoneal/perivertebral veins. Inferior mesenteric collaterals communicate with retroperitoneal veins and hemorrhoidal veins. As mentioned earlier, as portal hypertension progresses, flow reversal occurs in isolated peripheral portal vein branches (Ralls, 1990; Wachsberg et al., 2002). It is very important to realize that most patients with portal hypertension maintain antegrade flow in

the main portal vein. In addition to reversed flow, slow flow that alternates between antegrade and retrograde is another sign of portal hypertension.

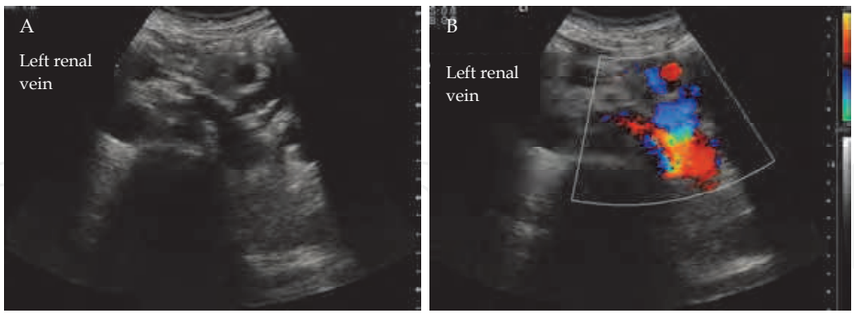

Fig. 29. Splenorenal shunt: [A] Dilated left renal vein; [B] Splenorenal shunt: splenic flow in blue going to the renal vein in red.

Portal vein thrombosis has been associated with chronic hepatitis, hepatocellular carcinoma, metastatic liver disease, carcinoma of the pancreas, chronic pancreatitis, septicemia, trauma, splenectomy, portocaval shunts and hypercoagulable states. Sonographic findings of portal vein thrombosis is best visualized in B-mode image and confirmed with color Doppler and include echogenic thrombus within the lumen of the vein, portal vein collaterals, expansion of the caliber of the vein and cavernous transformations. Cavernous transformation of the portal vein refers to numerous wormlike vessels at the porta hepatis, which represent periportal collateral circulation. Acute thrombus may appear relatively anechoic and may be overlooked unless Doppler interrogation is performed. Malignant thrombosis of the portal vein has a high association with HCC and is often expansive. Doppler sonography is useful in distinguishing between benign and malignant portal vein thrombi in patients with cirrhosis. Both benign and malignant thrombi may demonstrate continuous blood flow. Pulsatile arterial flow has been found to be 95% specific for the diagnosis of malignant portal vein thrombosis (Fig.18F). The sensitivity was only 62% because many malignant thrombi can be hypovascular (Dodd et al., 1995).

The normal hepatic artery in a fasting patient has a low resistance Doppler flow profile with an expected RI ranging from 0.55 to 0.7 (Fig.30A). During systole, the velocity is approximately 30-60 cm/sec; while during diastole, it normally slows to approximately 10-20 cm/sec, which is normally less than the velocity of the portal vein flow. The systolic acceleration time is typically less than 0.07 s. Liver disease may manifest in the hepatic artery as abnormally elevated (RI >0.7) or decreased (RI <0.55) resistance. High resistance is a nonspecific finding that may be seen in the postprandial state, patients of advanced age, and diffuse peripheral microvascular compression or disease, as seen in chronic hepatocellular disease including cirrhosis, hepatic venous congestion, cold ischemia (posttransplantation) and any stage of transplant rejection (Martínez-Noguera et al., 2002). The effect of cirrhosis on hepatic arterial microcirculation is complex and variable. Arterial resistance has been shown to be decreased, normal, or increased in cirrhotic patients (Vassiliades et al., 1993). Some aspects of the disease process, such as inflammatory edema, arterial compression by regenerative nodules and arterial compression by stiff noncompliant (fibrotic) parenchyma, have been thought to increase resistance (Fig.30B) (Alpern et al., 1987; Sacerdoti et al., 1995). Other aspects, such as the "hepatic arterial buffer response" (compensatory small artery proliferation and increased numbers of arteriolar beds) and

arteriovenous shunting, are thought to decrease resistance (Lautt & Greenway, 1987). The overall balance of these factors presumably dictates the observed resistance, and it has been shown that hepatic arterial RI is not useful for diagnosing cirrhosis or predicting its severity (Lim et al., 2005; Vassiliades et al., 1993). It is important to compare the resistive indexes to those from prior examinations of the same patient.

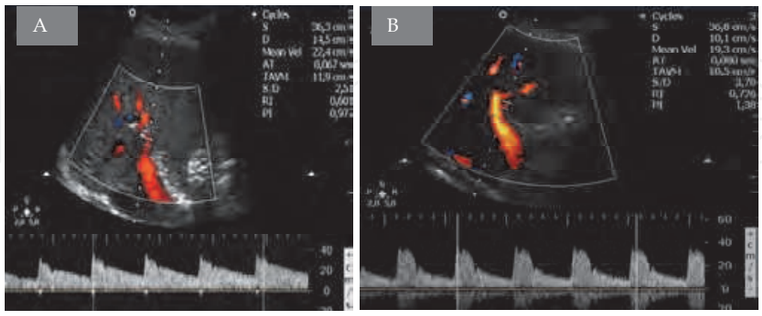

Fig. 30. HEPATIC ARTERY: [A] Normal low resistance flow in hepatic artery; [B] High resistance flow seen in the hepatic artery of the cirrhotic patient.

3.5 Liver transplantation

Liver transplantation has rapidly advanced from an experimental therapy to a mainstream treatment option for a wide range of acute and chronic liver diseases. Indications for liver transplant have evolved to include previously contraindicated conditions such as hepatocellular carcinoma and alcohol-related liver disease. Cirrhosis from chronic hepatitis C infection remains the most common indication today. The progressive improvement in survival from liver transplantation over the past few years has been due to a combination of factors, including better patient selection, improved organ preservation, developments in surgical technique, modern immunosuppressive agents and improved postoperative management. Overall posttransplant outcomes have steadily improved, with unadjusted 5-year patient survival rates of 77% among patients transplanted with MELD (Model for End-Stage Liver Disease) score between 15 and 20, and 72% for those with MELD scores between 21 and 30 (Merion, 2010). Ultrasound plays an important role in patient selection and management, being used in the pre-operative, operative and postoperative periods.

4. Conclusion

In conclusion, US imaging is an ideal complementary diagnostic tool to evaluate the liver from bench to bedside. Hepatic US can examine the internal architecture of the liver parenchyma, biliary system, portal and hepatic vascular supply. US can be regarded as a noninvasive method valid for follow-up studies of experimental hepatic diseases in rodents for pre-clinical drug or cell based therapy. Also, is the test of choice for assessment and follow-up of patients with suspected diffuse or focal hepatic disease, portal hypertension and screening for vascular and biliary complications following liver transplantation.

5. References

Alpern, M.B.; Rubin, J.M.; Williams, D.M. & Capek, P. (1987). Porta hepatis: duplex Doppler US with angiographic correlation. *Radiology,* Vol. 162, (January 1987), pp. 53–56.

Arai, K.; Matsui, O.; Takashima, T.; Ida, M. & Nishida, Y. (1988). Focal spared areas in fatty liver caused by regional decreased portal flow. *AJR American Journal of Roentgenology*, Vol. 151, No. 2, (August 1988), pp. 300–302.

Baker, M.K.; Wenker, J.C.; Cockerill, E.M. & Ellis, J.H. (1985). Focal fatty infiltration of the liver: diagnostic imaging. *Radiographic*s, Vol. 5, No. 6, (November 1985); pp. 923–929.

Biller, D.S.; Kantrowitz, B. & Miyabayashi, T. (1992). Ultrasonography of diffuse liver disease. A review. *Journal of Veterinary Internal Medicine*, Vol. 6, No. 2, (March-April 1992), pp. 71-76.

Bolondi, L.; Gandolfi, L.; Arienti, V.; Caletti, G.C.; Corcioni, E.; Gasbarrini, G. & Labò, G. (1982). Ultrasonography in the diagnosis of portal hypertension: diminished response of portal vessels to respiration. *Radiology*, Vol. 142, No. 1, (January 1982), pp. 167-172.

Bolondi, L.; Sofia, S.; Siringo, S.; Gaiani, S.; Casali, A.; Zironi, G.; Piscaglia, F.; Gramantieri, L.; Zanetti, M. & Sherman, M. (2001). Surveillance programme of cirrhotic patients for early diagnosis and treatment of hepatocellular carcinoma: a cost effectiveness analysis. *Gut,* Vol. 48, No. 2, (February 2001), pp. 251-259.

Brown, J.J.; Naylor, M.J. & Yagan, N. (1997). Imaging of hepatic cirrhosis. *Radiology*, Vol. 202, No. 1, (January 1997), pp. 1–16.

Burcharth, F. (1979). Percutaneous transhepatic portography. Technique and application. *AJR American Journal of Roentgenology*, Vol. 132, No. 2, (February 1979), pp. 177-182.

Caturelli, E.; Pompili, M.; Bartolucci, F.; Siena, D.A.; Sperandeo, M.; Andriulli, A.; Bisceglia, M. (2001). Hemangioma-like lesions in chronic liver disease: Diagnostic evaluation in patients. *Radiology*, Vol. 220, No. 2, (August 2001), pp. 337-342.

Choi, Y.J.; Baik, S.K.; Park, D.H.; Kim, M.Y.; Kim, H.S.; Lee, D.K.; Kwon, S.O.; Kim, Y.J. & Park, J.W. (2003). Comparison of Doppler ultrasonography and the hepatic venous pressure gradient in assessing portal hypertension in liver cirrhosis. *Journal of Gastroenterology and Hepatolology*, Vol. 18, No. 4, (April 2003), pp. 424-429.

Dias, J.V.; Paredes, B.D.; Mesquita, L.F.Q.; Carvalho, A.B.; Koslowski, E.O.; Lessa, A.S.; Takiya, C.M.; Resende, C.M.C.; Coelho, H.S.M.; Campos-de-Carvalho, A.C.; Rezende, G.F.M. & Goldenberg, R.C.S. (2008). An ultrasound and histomorphological analysis of experimental liver cirrhosis in rats. *Brazilian Journal of Medical and Biological Research*, Vol. 41, No. 11, (November 2008), pp. 992-999, ISSN 0100-879X.

Dodd, G.D.; Memel, O.S.; Baron, R.L.; Eichner, L. & Santiguida, L.A. (1995). Portal vein thrombosis in patients with cirrhosis. Does sonographic detection of intrathrombus flow allow differentiation of benign and malignant thrombus? *AJR American Journal of Roentgenology*, Vol. 165, No. 3, (September 1995), pp. 573-577.

Edmonson, H.A. & Craig, J.R. (1987). Neoplasms of the liver, In: *Diseases of the Liver*, L. Shiff & E.R. Shiff, (Eds.), 1147-1150, Lippincott, Philadelphia, USA.

El-Hassan, A.Y.; Ibrahim, E.M.; Al-Mulhim, F.A.; Nabhan, A.A. & Chammas, M.Y. (1992). Fatty infiltration of the liver: analysis of prevalence, radiological and clinical features and influence on patient management. *British Journal of Radiology*, Vol. 65, No.777 , (September 1992), pp.774-778.

Gibson, R.N.; Gibson, P.R.; Donlan, J.D. & Clunie, D.A. (1989). Identification of a patent paraumbilical vein by using Doppler sonography: importance in diagnosis of portal

hypertension. *AJR American Journal of Roentgenology*, Vol. 153, No. 3, (September 1989), pp. 513-516.

Giorgio, A.; Amoroso, P.; Lettieri, G.; Fico, P.; De Stefano, G.; Finelli, L.; Scala, V.; Tarantino, L.; Pierri, P. & Pesce, G. (1986). Cirrhosis: value of caudate to right lobe ratio in diagnosis with US. *Radiology*, Vol. 161, No. 2, (November 1986), pp. 443-445.

Haag, K.; Rossle, M.; Ochs, A.; Huber, M.; Siegerstetter, V.; Olschewski, M.; Berger, E.; Lu, S. & Blum, H.E. (1999). Correlation of duplex sonography findings and portal pressure in 375 patients with portal hypertension. *AJR American Journal of Roentgenology*, Vol. 172, No. 3, March 1999), pp. 631-635.

Harbin, W.P.; Robert, N.J. & Ferrucci, J.T. (1980). Diagnosis of cirrhosis based on regional changes in hepatic morphology: a radiological and pathological analysis. *Radiology*, Vol. 135, No. 2, (May 1980), pp. 273-83.

Lafortune, M.; Marleau, D.; Breton, G.; Viallet, A.; Lavoie, P. & Huet, P.M. (1984). The portal venous system measurements in portal hypertension. *Radiology*, Vol. 151, No. 1, (April 1984), pp. 27-30.

Lautt, W.W. & Greenway, C.V. (1987). Conceptual review of the hepatic vascular bed. *Hepatology*, Vol. 7, No. 5, (September-October 1987), pp. 952–963.

Lee, G.P.; Jeong, W.I.; Jeong, D.H.; Do, S.H.; Kim, T.H. & Jeong, K.S. (2005). Diagnostic evaluation of carbon tetrachloride-induced rat hepatic cirrhosis model. *Anticancer Research*, Vol. 25, No. 2A, (March/April 2005), pp.1029-38.

Lessa, A.S.; Rezende, G.F.M. & Resende, C.M. (2008). Ultra-sonografia na avaliação de um modelo experimental de esteatose e cirrose em ratos Wistar. *Radiologia Brasileira*, Vol. 41, No. 2, (March/April 2008), pp. 98.

Lessa, A.S.; Paredes, B.D.; Dias, J.V.; Carvalho, A.B.; Quintanilha, L.F.; Takiya, C.M.; Tura, B.R.; Rezende, G.F.M.; Campos de Carvalho, A.C.; Resende, C.M. & Goldenberg, R.C. (2010). Ultrasound imaging in an experimental model of fatty liver disease and cirrhosis in rats. *BMC Veterinary Research*, Vol. 6, (January 2010), pp. 1-10. Available from: http://www.biomedcentral.com/1746-6148/6/6

Levine, E.; Cook, L.T. & Granthem, J.J. (1985). Liver cysts in autosomal-dominant polycystic kidney disease. Clinical and computed tomographic study. *AJR American Journal of Roentgenology*, Vol. 145, No. 2, (August 1985), pp. 229-233.

Lewall, D.B. & McCorkell, S.J. (1985). Hepatic echinococcal cysts: Sonographic appearance and classification. *Radiology*, Vol. 155, No. 3, (June 1985), pp. 773-775.

Lima, V.M.; Oliveira, C.P.; Alves, V.A.; Chammas, M.C.; Oliveira, E.P.; Stefano, J.T. Mello, E.S.; Cerri, G.G.; Carrilho, F.J. & Caldwell, S.H.J. (2008). A rodent model of NASH with cirrhosis, oval cell proliferation and hepatocellular carcinoma. *Hepatology*, Vol. 49, No. 6, (December 2008), pp. 1055-1061.

Lim, A.K.; Patel, N.; Eckersley, R.J.; Kuo, Y.T.; Goldin, R.D.; Thomas, H.C.; Cosgrove, D.O.; Taylor-Robinson, S.D. & Blomley, M.J. (2005). Can Doppler sonography grade the severity of hepatitis C-related liver disease? *AJR American Journal of Roentgenology*, Vol. 186, No. 6, (June 2005), pp. 1848–1853.

Lorenz, J. & Winsberg, F. (1996). Focal hepatic vein stenoses in diffuse liver disease. *Journal of Ultrasound in Medicine,* Vol. 15, No. 4, (April 1996), pp. 313-316.

Mannheimer, E.G.; Quintanilha, L.F.; Carvalho, A.B.; Paredes, B.D.; Carvalho, F.G.; Takyia, C.M.; Resende, C.M.; Rezende, G.F.M.; Campos-de-Carvalho, A.C., Schanaider, A. & Goldenberg, R.C.S. (2011). Bone marrow cells obtained from cirrhotic rats do not

improve function or reduce fibrosis in a chronic liver disease model. *Clinical Transplantation*, Vol. 25, No. 1, (January 2011), pp. 54-60.

Martínez-Noguera, A.; Montserrat, E.; Torrubia, S. & Villalba, J. (2002). Doppler in hepatic cirrhosis and chronic hepatitis. *Seminars in Ultrasound, CT, and MR*, Vol. 23, No. 1, (February 2002), pp. 19–36.

Matsui, O.; Kadoya, M.; Takahashi, S.; Yoshikawa ,J.; Gabata, T.; Takashima, T. & Kitagawa, K. (1995). Focal sparing of segment IV in fatty livers shown by sonography and CT: correlation with aberrant gastric venous drainage. *AJR American Journal of Roentgenology*, Vol. 164, No. 5, (May 1995), pp. 1137–1140.

Merion, R.M. (2010). Current Status and Future of Liver Transplantation. *Seminars in Liver Disease*, Vol. 30, No. 4, (November 2010), pp. 411-421.

Moriyasu, F.; Nishida, O.; Ban, N.; Nakamura, T.; Sakai, M.; Miyake, T. & Uchino, H. (1986). Congestion index of the portal vein. *AJR American Journal of Roentgenology*, Vol. 146, No. 4, (April 1986), pp. 735-739.

Nunez, D. Jr; Russell, E.; Yrizarry, J.; Pereiras, R. & Viamonte, M. Jr. (1978). Portosystemic communications studied by transhepatic portography. *Radiology*, Vol. 127, No. 1, (April 1978), pp. 75-79.

Ohta, M.; Hashizume, M.; Kawanaka, H.; Akazawa, K.; Tomikawa, M.; Higashi, H.; Kishihara, F.; Tanoue, K. & Sugimachi, K. (1995). Prognostic significance of hepatic vein waveform by Doppler ultrasonography in cirrhotic patients with portal hypertension. *American Journal of Gastroenterology,* Vol. 90, No. 10, (October 1995), pp. 1853-1857.

Palmentieri, B.; De Sio, I.; La Mura, V.; Masarone, M.; Vecchione, R.; Bruno, S.; Torella, R. & Persico, M. (2006). The role of bright liver echo pattern on ultrasound B-mode examination in the diagnosis of liver steatosis. *Digestive and Liver Disease*, Vol. 38, No. 7, (July 2006), pp. 485-489.

Parkin, D.M.; Bray, F.; Ferlay, J. & Pisani, P. (2005). Global cancer statistics, 2002. *CA: A Cancer Journal for Clinicians,* Vol. 55, No. 2, (March-April 2005), pp. 74–108.

Partington, B.P. & Biller, D.S. (1995). Hepatic Imaging with radiology and ultrasound. *Veterinary Clinics of North America: Small Animal Practice*, Vol. 25, No. 2, (March 1995), pp. 305-335.

Ralls, P.W.; Barnes, P.F.; Radin, D.R.; Colletti, P. & Halls, J. (1987). Sonographic features of amebic and pyogenic liver abscesses: A blinded comparison. *AJR American Journal of Roentgenology,* Vol. 149, No. 3, (September 1987), pp. 499-501.

Ralls, P.W.; Barnes, P.F.; Johnson, M.B., De Cock, K.M.; Radin, D.R. & Halls, J. (1987). Medical treatment of hepatic amebic abscess: Rare need for percutaneous drainage. *Radiology*, Vol. 165, No. 3, (December 1987), p. 805-807.

Ralls, P.W. (1990). Color Doppler sonography of the hepatic artery and portal venous system. *AJR American Journal of Roentgenology*, Vol. 155, No. 3, (September 1990), pp. 517-525.

Redston, M.S. & Wanless, I.R. (1996). The hepatic von Meyenburg complex: Prevalence and association with hepatic and renal cysts among 2843 autopsies. *Modern Pathology*, Vol. 9, No. 3, (March 1996), p. 233-237.

Sacerdoti, D.; Merkel, C.; Bolognesi, M.; Amodio, P.; Angeli, P. & Gatta, A. (1995). Hepatic arterial resistance in cirrhosis with and without portal vein thrombosis: relationships with portal hemodynamics. *Gastroenterology*, Vol. 108, No. 4, (April 1995), pp. 1152–1158.

Sangiovanni, A.; Del Ninno, E.; Fasani, P.; De Fazio, C.; Ronchi, G.; Romeo, R.; Morabito, A.; De Franchis, R.; Colombo, M. (2004). Increased survival of cirrhotic patients with a hepatocellular carcinoma detected during surveillance. *Gastroenterology*, Vol. 126, No. 4, (April 2004), pp. 1005-1014.

Snover, D.C. (2009). Non-neoplastic liver disease, In: *Sternberg's diagnostic surgical pathology*, E.C. Mills, D. Carter, J.K. Greeson, (Eds.), 1167-1191, Lippincott Williams & Wilkins, Philadelphia, USA.

Tanaka, S.; Kitamura, T.; Fujita, M.; Nakanishi, K. & Okuda, S. (1990). Color Doppler flow imaging of liver tumors. *AJR American Journal of Roentgenology*, Vol. 154, No. 3, (March 1990), pp. 509-514.

Taylor, K.J.W.; Riely, C.A.; Hammers, L.; Flax, S.; Weltin, G.; Garcia-Tsao, G.; Conn, H.O.; Kuc, R. & Barwick, K.W. (1986). Quantitative US attenuation in normal liver and in patients with diffuse liver disease: importance of fat. *Radiology*, Vol. 160, No. 1, (July 1986), pp. 65–71.

Vassiliades, V.G.; Ostrow, T.D.; Chezmar, J.L.; Hertzler, G.L. & Nelson RC. (1993). Hepatic arterial resistive indices: correlation with the severity of cirrhosis. *Abdominal Imaging*, Vol. 18, No. 1, (1993), pp. 61–65.

Wachsberg, R.H. & Simmons, M.Z. (1994). Coronary vein diameter and flow direction in patients with portal hypertension: evaluation with duplex sonography and correlation with variceal bleeding. *American Journal of Gastroenterology*, Vol. 162, No. 3, (March 1994), pp. 637-641.

Wachsberg, R.H.; Bahramipour, P.; Sofocleous, C.T. & Barone, A. (2002). Hepatofugal flow in the portal venous system: pathophysiology, imaging findings, and diagnostic pitfalls. *Radiographics,* Vol. 22, No. 1, (January-February 2002), pp. 123-140.

Wanless, I.R. & Lentz, J.S. (1990). Fatty liver hepatitis (steatohepatitis) and obesity: an autopsy study with analysis of risk factors. *Hepatology*, Vol. 12, No. 5, (November 1990), pp. 1106–1110.

Weinreb, J.; Kumari, S.; Phillips, G. & Pochaczevsky R. (1982). Portal vein measurements by real time sonography. *AJR American Journal of Roentgenology*, Vol. 139, No. 3, (September 1982), pp. 497-499.

Wernecke, K.; Vassallo, P.; Bick, U.; Diederich, S. & Peters, P.E. (1992). The distinction between benign and malignant liver tumors on sonography: Value of a hypoechoic halo. *AJR American Journal of Roentgenology*, Vol. 159, No. 5, (November 1992), pp. 1005-1009.

WHO: The World Health Report 2004 – changing history – deaths by cause, sex and mortality stratum in WHO regions, estimates for 2002, Published 2004, Accessed December 15 2010, Available from:
http://www.who.int/whr/2004/annex/topic/en/annex_2_en.pdf.

Wilson, S.R. & Withers, C.E. (2005). The liver. In: *Diagnostic ultrasound*, C.R. Rumack, J.A. Wilson, J.W. Charboneau, (Eds.), 77-145, Elsevier Mosby, St Louis, USA.

Zironi, G.; Gaiani, S.; Fenyves, D.; Rigamonti, A.; Bolondi, L. & Barbara, L. (1992). Value of measurement of mean portal flow velocity by Doppler flowmetry in the diagnosis of portal hypertension. Journal of Hepatology, Vol. 16, No. 3, (November 1992), pp. 298-303.

Zwiebel, W.J. (1995). Sonographic diagnosis of diffuse liver disease. Seminars in Ultrasound, CT and MRI, Vol. 16, No. 1, (February 1995), pp. 8–15.

Ultrasound Imaging - Medical Applications

Edited by Prof. Oleg Minin

ISBN 978-953-307-279-1
Hard cover, 330 pages
Publisher InTech
Published online 23, August, 2011
Published in print edition August, 2011

This book provides an overview of ultrafast ultrasound imaging, 3D high-quality ultrasonic imaging, correction of phase aberrations in medical ultrasound images, etc. Several interesting medical and clinical applications areas are also discussed in the book, like the use of three dimensional ultrasound imaging in evaluation of Ashermanâ€™s syndrome, the role of 3D ultrasound in assessment of endometrial receptivity and follicular vascularity to predict the quality oocyte, ultrasound imaging in vascular diseases and the fetal palate, clinical application of ultrasound molecular imaging, Doppler abdominal ultrasound in small animals and so on.

How to reference

In order to correctly reference this scholarly work, feel free to copy and paste the following:

Celia Resende, Andréia Lessa and Regina C. S. Goldenberg (2011). Ultrasonic Imaging in Liver Disease: From Bench to Bedside, Ultrasound Imaging - Medical Applications, Prof. Oleg Minin (Ed.), ISBN: 978-953-307-279-1, InTech, Available from: http://www.intechopen.com/books/ultrasound-imaging-medical-applications/ultrasonic-imaging-in-liver-disease-from-bench-to-bedside

INTECH
open science | open minds

InTech Europe
University Campus STeP Ri
Slavka Krautzeka 83/A
51000 Rijeka, Croatia
Phone: +385 (51) 770 447
Fax: +385 (51) 686 166
www.intechopen.com

InTech China
Unit 405, Office Block, Hotel Equatorial Shanghai
No.65, Yan An Road (West), Shanghai, 200040, China
中国上海市延安西路65号上海国际贵都大饭店办公楼405单元
Phone: +86-21-62489820
Fax: +86-21-62489821

IntechOpen